

**UNIVERSITY OF GAZIANTEP
GRADUATE SCHOOL OF
NATURAL & APPLIED SCIENCES**

**INTERNAL CURING OF HIGH STRENGTH
CONCRETE BY USING COLD BONDED
AGGREGATES**

**M. Sc. THESIS
IN
CIVIL ENGINEERING**

**by
ALI NOORULDEEN ISMAEL**

MAY 2014

Internal Curing of High Strength Concretes by Using Cold Bonded Aggregates

**M.Sc. Thesis
in
Civil Engineering
University of Gaziantep**

**Supervisor
Assoc. Prof. Dr. Mehmet GESOĞLU**

**by
Ali Nooruldeen ISMAEL**

May 2014

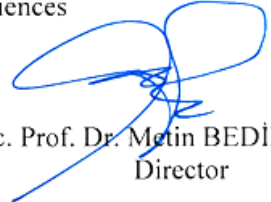
© 2014 [Ali Nooruldeen ISMAEL]

T.C.
UNIVERSITY OF GAZİANTEP
GRADUATE SCHOOL OF
NATURAL & APPLIED SCIENCES
CIVIL ENGINEERING DEPARTMENT

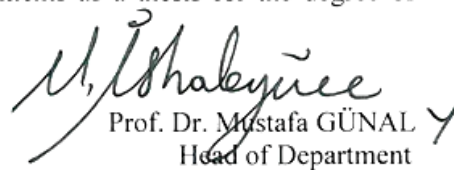
Name of the thesis: Internal curing of very high strength concretes by using cold bonded aggregates

Name of the student: Ali Nooruldeen ISMAEL
Exam date: May, 2014


Approval of the Graduate School of Natural and Applied Sciences


Assoc. Prof. Dr. Metin BEDİR
Director

I certify that this thesis satisfies all the requirements as a thesis for the degree of Master of Science.


Prof. Dr. Mustafa GÜNAL
Head of Department

This is to certify that we have read this thesis and that in our opinion it is fully adequate, in scope and quality, as a thesis for the degree of Master of Science.


Assoc. Prof. Dr. Mehmet GESOĞLU
Supervisor

Examining Committee Members

Signature

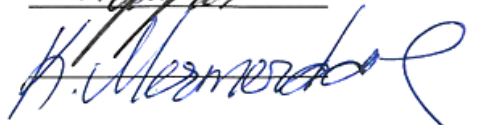
Assoc. Prof. Dr. Mehmet GESOĞLU



Assoc. Prof. Dr. Erhan GÜNEYİSİ



Assist. Prof. Dr. Kasım MERMERDAŞ





I hereby declare that all information in this document has been obtained and presented in accordance with academic rules and ethical conduct. I also declare that, as required by these rules and conduct, I have fully cited and referenced all material and results that are not original to this work.

Ali Nooruldeen ISMAEL

ABSTRACT

INTERNAL CURING OF HIGH STRENGTH CONCRETE BY USING COLD BONDED AGGREGATES

ISMAEL, Ali Nooruldeen

M.Sc. in Civil Engineering

Supervisor: Assoc. Prof. Dr. Mehmet GESOĞLU

May 2014, Page 88

This study aims at examining experimentally the shrinkage and mechanical properties of High-Strength Concrete (HSC) containing blast furnace slag aggregates (ASA) and artificial fly ash aggregates (AFA) that are employed as water reservoirs to enable internal curing. So as to form fly ash and/or slag aggregates, a dry powder blend of 10% of Portland cement and 90% fly ash or slag was initially pelletized by moisturizing at room temperature in a spinning skewed pan; these were subsequently cured for 28 day. Applying a 0.28 water-to-cement ratio, nine HSCs mixtures were developed with different ASA or AFA replacement levels, i.e. 0%, 5%, 10%, 15%, and 20%. After 28 day, testing of the hardened concretes was conducted for splitting tensile strength, compressive strength, and modulus of elasticity. The concrete was monitored for a 57 day drying period to determine the restrained shrinkage, autogenous shrinkage, and drying shrinkage along with the water loss. The HSCs having 20% ASAs showed the highest mechanical properties. Additionally, HSCs containing ASA showed a longer cracking period of the concretes causing finer cracks that are linked to the lower free shrinkage. Largely in the HSCs containing 20% AFA, there was, however, a noticeable decline in the autogenous shrinkage for all the HSCs with AAs, especially for HSCs with 20% AFA.

Keywords: Artificial aggregate, High strength concrete, Autogenous shrinkage, Drying shrinkage, Restrained shrinkage.

ÖZET

YÜKSEK DAYANIMLI BETONUN SOĞUK BAĞLAMA YÖNTEMİYLE ÜRETİLEN AGREGALAR İLE İÇSEL KÜRLENMESİ

ISMAEL, Ali Nooruldeen

İnşaat Mühendisliği Yüksek Lisans

Danışman: Doç. Dr. Mehmet GESOĞLU

Mayıs 2014, Sayfa 88

Bu tezde, içsel kürü sağlamak amacıyla su rezervuarı olarak kullanılan yapay uçucu kül (AFA) ve yapay yüksek fırın cürufu agregalarını (ASA) içeren yüksek dayanımlı betonların (HSC) rötre çatlağı oluşumuna karşı performansı deneysel olarak incelenmiştir. Yapay agregalar, %90 uçucu kül veya cüruf ile %10 çimentonun soğuk bağlanarak peletlenmesiyle üretilmiştir. AFA ve ya ASA agregaların toplam agrega hacminin %0, %5, %10, %15 ve %20 oranlarında kullanılmasıyla, su-çimento oranı 0.28 olan toplam dokuz adet beton karışımı tasarlanmıştır. Sertleşmiş betonların, 28 günlük mekanik özellikleri, basınç dayanımı, yarmada çekme dayanımı, elastisite modülü testleri ile ölçülmüştür. Ek olarak, kuruma rötresi, ağırlık kaybı, sınırlandırılmış rötre çatlağı ve otojen rötre 57 gün boyunca gözlemlenmiştir. Test sonuçlarına göre en iyi mekanik özellikler %20 ASA içeren HSC’de elde edilmiştir. ASA kullanılması HSC’lerin çatlama zamanlarını uzatmış ve ince çatlaklarla birlikte azalan kuruma rötresi ile sonuçlanmıştır. Bunların dışında, yapay agrega içeren HSC’lerde otojen rötre önemli miktarda azalmıştır.

Anahtar kelimeler: Yapay agrega; Otojen rötre; Kuruma rötresi; Yüksek dayanımlı beton; Sınırlandırılmış rötre.

To my parents, wife and daughter

ACKNOWLEDGEMENTS

In the name of Allah, the Most Benevolent, the most Merciful. First of all, I wish to record immeasurable gratitude and thankful fullness to the One and The Almighty Creator, the Lord and Sustainer of the universe, and the Mankind, in particular. It is only through His mercy and help that this work could be completed, and it is ardently desired that this little effort be accepted by Him to be of some service to the cause of humanity.

I would like to take this opportunity to express my gratitude to my supervisor Assoc. Prof. Dr. Mehmet GESOĞLU for his constant guidance and encouragement.

A special thank to University of Gaziantep for the real support and laboratory facilities. I don't forget to thank Assoc. Prof. Dr. Erhan GÜNEYİSİ; for his encouraging, supporting, advice me and care about my work. Special thank to Research Asst. Hatice Öznur ÖZ, she who was directly or indirectly involved in the process of producing this research report, for her generous assistance.

To all my friends, for their support and giving me a suitable environment to study, and for the nice and useful moments I spend with them.

CONTENTS

ABSTRACT.....	v
ÖZET.....	vi
DEDICATION.....	vii
ACKNOWLEDGMENTS	viii
TABLE OF CONTENTS.....	ix
LIST OF TABLES	xii
LIST OF FIGURES	xiii
LIST OF SYMBOLS/ABBREVIATIONS.....	xvi
CHAPTER 1: INTRODUCTION.....	1
1.1 General.....	1
1.2 Research Objective.....	3
1.3 Thesis Organaztion.....	4
CHAPTER 2: LITERATURE REVIEW AND BACKGROUND.....	5
2.1. Introduction.....	5
2.2. High Strength Concrete (HSC).....	5
2.3. Ingredient materials for high strength concrete.....	7
2.3.1. Cement.....	7
2.3.2. Water-cement ratio.....	7
2.3.3. Aggregates.....	8
2.3.3.1 Coarse aggregate.....	8
2.3.3.2 Fine aggregate.....	9

2.3.4 Admixtures.....	10
2.3.4.1 Chemical admixtures.....	10
2.4. Fly Ash.....	12
2.5. Ground Granulated Blast-Furnace Slag (GGBFS).....	14
2.6. Pelletizing Process.....	16
2.6.1. Definition.....	16
2.6.2 Pelletization Mechanisms.....	18
2.7 Bonding between Cement Paste and Aggregate.....	22
2.8 Shrinkage in Concrete.....	25
2.8.1 Autogenous Shrinkage.....	26
2.8.2 Drying Shrinkage.....	27
2.9 Mechanisms of Shrinkage.....	29
2.10 Internal Curing Overview.....	32
2.11 Method to Incorporate Water in Concrete.....	34
CHAPTER 3: EXPERIMENTAL PROGRAM AND METHODOLGY.....	37
3.1. Introduction.....	37
3.2. Materials.....	38
3.2.1.Cement.....	38
3.2.2. Fly Ash.....	38
3.2.3. Ground Granulated Blast Furnace Slag.....	39
3.2.4. Superplasticizer.....	39
3.2.5. Aggregates.....	39
3.2.5.1. Artificial Cold-Bonded Aggregates.....	39
3.2.5.2. Natural Aggregates.....	43
3.3. Concrete Mixture Details.....	44

3.4. Concrete Casting and Curing.....	47
3.5 Tests for Mechanical Properties.....	51
3.5.1. Compressive Strength.....	51
3.5.2. Modulus of Elasticity.....	51
3.5.3. Splitting Tensile Strength.....	52
3.6. Tests for Physical Properties.....	53
3.6.1. Drying Shrinkage and Weight Loss.....	53
3.6.2. Autogenous Shrinkage.....	54
3.6.3. Restrained Shrinkage Cracking.....	56
3.7. Microstructural Analysis.....	58
CHAPTER 4: TEST RESULTS AND DISCUSSIONS.....	59
4.1. Fresh Concrete Density.....	59
4.2. Microstructural Characteristics of ASA and AFA.....	59
4.3. Mechanical Properties.....	63
4.3.1 Compressive Strength.....	63
4.3.2 Splitting tensile strength.....	65
4.3.3 Modulus of Elasticity.....	65
4.4 Physical Properties.....	67
4.4.1 Drying Shrinkage and Weight Loss.....	67
4.4.2 Linear Autogenous Shrinkage.....	70
4.4.3 Restrained shrinkage cracking.....	72
CHAPTER 5: CONCLUSIONS.....	74
REFERENCES.....	76

LIST OF TABLES

Table 3.1 Physical and chemical properties of Cement, Fly Ash and Slag.....	38
Table 3.2 Properties of Superplasticizer.....	39
Table 3.3 Sieve analysis and physical properties of natural and artificial aggregates.....	44
Table 3.4 Aggregates volume fractions for artificial coarse aggregates.....	45
Table 3.5 Concrete mixture proportions in kg/m ³	46
Table 4 Drying, autogenous and restrained shrinkage performance with fresh density of HSCs.....	68

LIST OF FIGURES

Figure 2.1 Dispersing action of water-reducing admixtures: (a)flocculated paste; (b)dispersed paste.....	12
Figure 2.2 Fly ash particles.....	14
Figure 2.3 Ground granulated blast furnace slag particles.....	16
Figure 2.4 Growing path of pellets.....	18
Figure 2.5 A schematic showing the driving force for pelletization due to reduction in total air-water interfacial area.....	19
Figure 2.6 Three main mechanisms of pellet formation and growth: nucleation, coalescence, and layering.....	20
Figure 2.7 Nuclei ball formation mechanism (water content below optimum state).....	22
Figure 2.8 Nuclei ball formation mechanism (water content above optimum state).....	22
Figure 2.9 Water loss versus time from concrete specimens of various sizes under 55% relative humidity.....	29
Figure 2.10 Representation of cement paste microstructure.....	30
Figure 2.11 LWA moisture transfer to hydrating cement paste.....	33

Figure 3.1 The general view of the pelletization disc.....	41
Figure 3.2 Artificial aggregate Self-curing process.....	42
Figure 3.3 Crushing strength test apparatus.....	42
Figure 3.4 Crushing load of the produced AAs.....	43
Figure 3.5 AAs in SSD condition.....	49
Figure 3.6 Plastic sheets inside the mold before the casting.....	49
Figure 3.7 a- Specimens sealed with two layers of plastic sheets. b-after plastic sheets specimens sealed with a layer of aluminum foil.....	50
Figure 3.8 The specimens in curing by water.....	50
Figure 3.9 Compressive strength test machine.....	51
Figure 3.10 Measuring of modulus of elasticity.....	52
Figure 3.11 Free shrinkage test a) Free shrinkage test set up and b) Test specimens...	54
Figure 3.12 a) Autogenous test specimens. b) Test apparatus.....	55
Figure 3.13 Autogenous deformation test set up for concrete specimens.....	55
Figure 3.14 The dimension of restrained shrinkage ring specimen.....	57
Figure 3.15 Restrained shrinkage test specimens.....	57
Figure 3.16 Photographic view of a cracked ring specimen.....	58

Figure. 4.1 SEM observation of HSCs (a) control mix (b) HSCs incorporating AFA (c) HSCs incorporating ASA.....	61
Figure.4.2 SEM-EDX for AFA0ASA0 and concretes.....	62
Figure 4.3 SEM-EDX for AFA20ASA0 concrete.....	62
Figure 4.4 SEM-EDX for AFA0ASA20 concrete.....	63
Figure 4.5 Variation of compressive/tensile strength of HSCs including AFA.....	66
Figure 4.6 Variation of compressive/tensile strength of HSCs including ASA.....	66
Figure 4.7 Variation of modulus of elasticity of all HSCs.....	67
Figure 4.8 Drying shrinkage for HSCs mixtures.....	69
Figure 4.9 Weight loss for HSCs mixtures.....	69
Figure 4.10 Autogenous shrinkage for HSCs contain ASAs & ASAs.....	71
Figure 4.11 Restrained shrinkage cracking of HSCs.....	73

LIST OF SYMBOLS/ ABBREVIATIONS

AA	Artificial aggregate
AASHTO	American Association of State Highway and Transportation Officials
ACI	American concrete institute
AFA	Artificial fly ash aggregate
ASA	Artificial slag aggregate
ASTM	American standard for testing material
BSI	British Standards Institution
C-S-H	Calcium-Silica-Hydrated (Gel)
EDX	Energy-dispersive X-ray spectroscopy
FA	Fly ash
FM	Fineness modulus
GGBFS	Ground granulated blast-furnace slag
HPC	High performance concrete
HSC	High strength concrete
IN	Internal Curing
ITZ	Interfacial transition zone
LWA	Lightweight aggregate

LWCA	Lightweight coarse aggregate
NCA	Natural coarse aggregate
NFA	Natural fine aggregate
NSC	Normal strength concrete
NWA	Normal weight aggregate
PC	Ordinary portland cement
SEM	Scanning electron microscopy
SP	Superplasticizer
SSD	Saturated surface dry aggregate
W/C	Water/cement ratio

CHAPTER 1

INTRODUCTION

1.1 General

In comparison to the conventional concrete, high-strength concrete (HSC) has more benefits. The high compressive strength is very beneficial in compression members such as columns and piles; it avails more floor space due to the resulting reduction in the necessary column size. In structures with large in-plane compressive stresses, the use of HSC is very effective, for example, folded plates, domes, arches, and shells. With HSC, the overall dead weight on a structure's foundation is reduced owing to the comparatively greater compressive strength per unit volume, per unit weight.

HSC is ordinarily characterized by low porosity and discontinuous capillary pore structure of the cement paste. This is mostly obtained by using a low water/cement ratio and high cement content with adding superplasticizers to HSC mixture to achieve the workability, that result high strength and impermeable concrete which it is important properties for concrete. Therefore, the volume of water in the concrete necessary for completion of the hydration process will be inadequate, while the water ingress will be hindered due to the impermeability of the concrete (Tasdemir et al., 2002 and Weber & Reinhardt, 1997). However, these types of concretes have also shown to be more sensitive to early-age cracking than traditional concrete (RILEM TC 181-EAS 2002).

The radius of the meniscus decreases due to the empty pores that form as a result of chemical shrinkage. This increases the capillary stress of the water in the pores leading to self-desiccation. At a constant temperature, the self-desiccation accompanied by water consumption by means of cement hydration in a closed system so as to ensure moisture is not lost, leads to autogenous deformation. Chemical shrinkage, on the other hand, enables fine pores to be formed and free water to be absorbed by the hydrates into the pores.

Conventional curing procedures of water ponding, as used for drying shrinkage, are not effective in the case of autogenous shrinkage. They may eliminate the autogenous shrinkage in small cross-sections only, because the penetration of water from the external surface is limited. Moreover, external curing might be difficult to apply to some surfaces. In view of this limitation, different strategies have been developed in recent years, based on the use of internal water reservoirs (RILEM TC-ICC 2002). One strategy, which has been investigated more extensively, is based on the use of lightweight aggregates (LWA) (Hammer, 1992), to prevent the shrinkage that results from self-desiccation and the associated drop in internal relative humidity, the minimum amount of water needed to supply internal curing is equal to the volume of water that is needed to fill the empty pore space that results from autogenous shrinkage associated with cement hydration, the method of internal curing with artificial aggregates (AA) using in the producing of HSC to act as a reserves to supply water for hydration process.

Internal curing is of particular use for preventing autogenous shrinkage in concrete, which reduces the internal relative humidity in the concrete so as to increase

shrinkage and early age cracking (Bentz and Snyder, 1999). Internal relative humidity is a measure of the amount of internal water that is available for cement hydration in the cement paste (Lura et. al., 2002).

1.2 Research Objectives

The aim of this study is to examine the properties of high strength concretes that contain cold bonded aggregate. The process of cold bonding at room temperature will be carried out to form artificial blast furnace slag and fly ash aggregate. While taking into consideration the fresh, shrinkage, and mechanical tests of the concretes, was subsequently replace the natural coarse aggregate in the High-Strength Concrete at a different replacement level. In the experiment, nine mixtures of HSCs were formed using 0.28 water-cement ratios and 570 kg/m³ total cement content. The main testing parameter important in cold bonded aggregates is the coarse aggregate volume fraction. Volume fractions of 5%, 10%, 15% and 20% of the entire coarse aggregate volume were chosen for the artificial aggregates. By use of slump test, workability was controlled. Compressive strength as well as the splitting tensile strength was examined to determine the concretes' hardened properties. Autogenous shrinkage, dry shrinkage, weight loss, and restrained shrinkage were also tested.

1.3 Thesis Organization

Chapter 1- Introduction: A brief introduction of the aim and objectives of this thesis is given.

Chapter 2- Literature review: Presents a literature review and overall background information regarding the high strength concrete. A brief definition and the pelletization process theory is outlined. Findings of previous studies on the concrete aggregate-cement paste interface bond characteristics are also summarized. The formation, structure, and properties of the mineral mixtures, i.e. ground granulated blast furnace slag (GGBFS) and fly ash are briefly introduced. Internal curing and shrinkage of concrete are also explained, giving brief background information.

Chapter 3-Experimental study: This includes a description of the materials, casting, mixtures, curing conditions, as well as test methods used.

Chapter 4-Test Results and Discussions: The study results are tabulated, assessed and discussed in this chapter.

Chapter 5- Conclusions: The conclusions drawn from the study findings are presented along with relevant recommendation for future research.

CHAPTER 2

LITERATURE REVIEW

2.1 Introduction

This part presents a literature review and general background information about HSCs requirements and material behavior are explained. A brief definition and theory of the Pelletization Process are presented. And also includes summary information about the concrete aggregate-cement paste interface bond characteristics through previous studies. Moreover, carrying out a brief introduction about the structure, formation, properties of mineral admixtures namely fly ash and ground granulated blast furnace slag (GGBFS) also shrinkage in concrete, mechanisms of shrinkage and internal curing in HSCs are discussed.

2.2 High strength concrete (HSC)

Concrete is composed mainly of cement paste and aggregates. The aggregates are found in the matrix of cement paste, besides pozzolans. According to (Berntsson et al., 1990), the components are crucial in concrete because the strength of concrete lies on their strength, deformation properties, and adhesion between the aggregate surface and paste. It is possible to make up to 120MPa compressive strength with natural aggregates. This is achieved through improving strength in cement paste and controlling it through the water-cement ratio and dosage of additional mixtures

(Mehta and Aitcin, 1990). Because of the advancing concrete technology, special superplasticizer, availability of chemicals and minerals, it is possible to produce concrete with strength of up to 100 MPa commercially. Besides, the concrete has acceptable variability levels by using ordinary aggregates (FIP/CEB, 1990). The developments have contributed to increased application of high-strength concrete (HSC) in the world. Variations in HSC strength are encountered at the bottom range in relation to the time and geographical location, availability of raw material, technology and demands in the industry. Consideration of concrete based on strength in the past 50 years is different from current considerations where low strength is recorded. For example, in 1950 is where production of concrete of 30 MPa was of high strength. In the years 1960, 1970 and 1980 respectively, a moderate compressive strength was witnessed. The strength witnessed is 40-50 MPa, 60 MPa and 100 MPa and they are used in practical structures. Despite of the growing developments in the concrete technology a concrete with 40-60 MPa strength is considered as HSC. From the North American practice (ACI 318, 1999), concrete with high strength meets the cylinder compressive strength of 41 MPa in 28 days. Contrasting this, state of the art report on high strength by (FIP/CIB 1990) recommends a high strength of 60 MPa on a 28 day cylinder compressive strength. According to (Carrasquillo, 1985), production of HSC does not require sophisticated materials rather it is accompanied with high quality materials in recommended proportions. The material selection of concrete depends on the HSC produced in relation to the requirements of the work and strength in development places in contrast to the lower strength concrete (ACI 363R, 2010). Additionally, trial batches are vital in generating data to help researchers and professionals in identification of optimum mix proportions of HSC. Practically examples drawn from mix proportion

of HSC used in already existing built structures is helpful information in getting HSC.

2.3 Ingredient materials for high strength concrete

2.3.1 Cement

The development of strength in the concrete relies on cement features and content. Using Portland cement for HSC is vital. Notably, there is no need of using Type-III cement if the high initial strength is not the objective for instance prestressed concrete. In cases where the temperature increase is a problem, a substitute of Type-II low heat of dehydration cement is used as long as it meets the strength requirements (ACI 363R, 2010).

In HSC without chemical admixture, a high cement content of 8 to 10 sacks is required. The content of the cement is based on the type of the cement: mainly 10 sacks/cu. Yd. for cement type-I and 9.25 sacks/cu. Yd. for cement type-II.

According to (Peterman and Carrasquillo, 1986), in HSC containing no chemical admixture, a high cement content of 8 to 10 sacks/cu. yd. must be used.

2.3.2 Water-cement ratio

Water-cement ratio is a vital variable in achievement of HSC (Peterman and Carrasquillo, 1986). When focusing on the production of HSC through conventional mixing technology, water-cement ratio of 0.22 to 0.40 is considered. Their

compressive strength is about 60 to 130 when there is use of normal density aggregates (FIP/CEB, 1990).

2.3.3 Aggregates

Aggregate properties do not contribute to the strength and modulus of elasticity of HSC. Considering the normal strength concrete (NSC), there is a tendency of aggregates having higher strength and stiffness than the normal cement paste. NSC failures results to fracturing of the cement and in the zones of transition between aggregate and paste. Additional the reduction in water-cement ratio results to improved compressive strength of cement paste and concrete.

2.3.3.1 Coarse aggregate (CA)

The limiting factor in HSC relies on the capacity of aggregate. This occurs when the aggregate is weaker than low water cement matrix. Besides it is not rigid enough in provision of enough strengthening effects in relation to the course aggregate (CA). To achieve optimum compressive strength having high cement content and low water-cement ratio then maximum size consideration is kept to minimum at 10 to 12 mm. The possibility increase in the strength is because of reduction in average bond stress due to surface area increase of aggregate. Additionally, smaller aggregate sizes contributes to the production of high strength concrete to less strong concentration of stress between particles as brought as a result of differences between the elastic moduli of the paste and the aggregate. From past studies, it is evident that production of higher strengths is characterized by crushed stones than rounded gravel. The reason attached to the effect is the greater mechanical bond that can develop together

with angular particles. However, the attendant high water requirements help in avoiding the accentuated angularity, water requirement and reduced workability. The requirements of ideal CA are cleanness, cubical, angular, and 100 percent of crushed containing a minimum of flat besides elongated particles (ACI 363R, 2010). The study of different aggregates indicates trap rock producing high strength concrete. Other crushed aggregates studied include quartzite, limestone, greywacke, granite and crushed level all producing low strength than trap rock but limestone produces more less the same as trap rock. Gradation of CA within ASTM has little effect in HSC strength. A ratio of coarse aggregate to fine aggregate leads to attainment of HSC optimum strength and workability. This is a recommendation for NSC. Besides, the high fine content of HSC mixes and use of ordinary proportions of CA resulting to a sticky mix (Peterman and Carrasquillo, 1986).

2.3.3.2 Fine aggregate (FA)

Other aggregate require less water mixture in concrete and hence recommended in HSC. Such aggregates are fine, circular in shape and smooth in texture. Additionally, the components of HSC include fine cementitious materials thus grading fine aggregates is not vital. Besides, the increase of fineness modulus (FM) as the lower FM of the fine aggregate makes the concrete sticky thus difficult to compact and less workable. It is recommended to use sand with a FM of 3.0 for HSC (ACI 363R, 2010).

2.3.4 Admixtures

Admixtures are materials used in the production of HSC. The materials are chemical, mineral admixtures and air entraining agents. The type of admixture chosen determines increase in compressive strength, accelerated strength gain, improved workability and durability. It is vital to put into consideration the reliable performance during selection.

2.3.4.1 Chemical admixtures

Use of certain admixtures for instance Superplasticizers result in increase in concrete strength through reducing the mixing water requirements of a constant slump and causes dispersal of cement particles. This may be accompanied with or without mixing water content thus resulting to efficient hydration. Use of Super plasticizers in concrete should be accompanied by high fine requirements for cohesiveness of the mixture besides slump loss. The HSC mixes contain sufficient fines because of high cement contents. Strength of the concrete can be improved by using retarders besides high doses and redoses of superplasticizers at the plant and the job site. It also helps in restoration of slump to initial amount. Additionally, stiff and difficult superplasticizers are vital in applied vibration (Peterman and Carrasquillo, 1986).

High range water reducers admixture (HRWRA) are simply water-soluble polymers with low molecular weight. Their main function is to reduce water from 12 to 30 percent in concrete mixtures with an aim of reaching a recommended slump (Gagne et al., 1996). The admixtures are mostly used in the production of high-strength concrete to 50 MPa, as there is a possibility of workable mixtures having as low as

0.40 water-cement ratios (Whiting and Dziedzic, 1979). The type of HRWRA chosen matters in relation with the economic demand and availability. There are chances of having an increase in compressive strength by usage of water admixtures in concrete mixtures, thus the increase can be visible early as one day in cases of low retardation. Notably, there are 25 percent compressive strength increases greater than expectation in decrease of water-cement ratios. Besides, it is also evident from uniform microstructure improvement in cement dispersal. HRWRA are used to reduce the permeability of concrete by creating uniform pore structure and reducing of water-cement ratio with aim of enhancing the cement durability (Ozyildirim, 2003).

Major opposing charges on adjacent particles in the cement paste causes electrostatic attractions thus flocculating of particles (figure 2.1a). To reduce the viscosity of paste and cement amount of water is considered in the agglomerates and absorbed on solid surfaces. Interactions occur between water molecules thus causing reduction to the reducing the admixture interaction to neutralize the surface charges to carry uniform charges of like. This result in the repulsion of particles instead of attraction remaining full dispersed in the paste (Figure 2.1b), hence water available reduces the viscosity of the paste and concrete (Mindess et al., 2003).

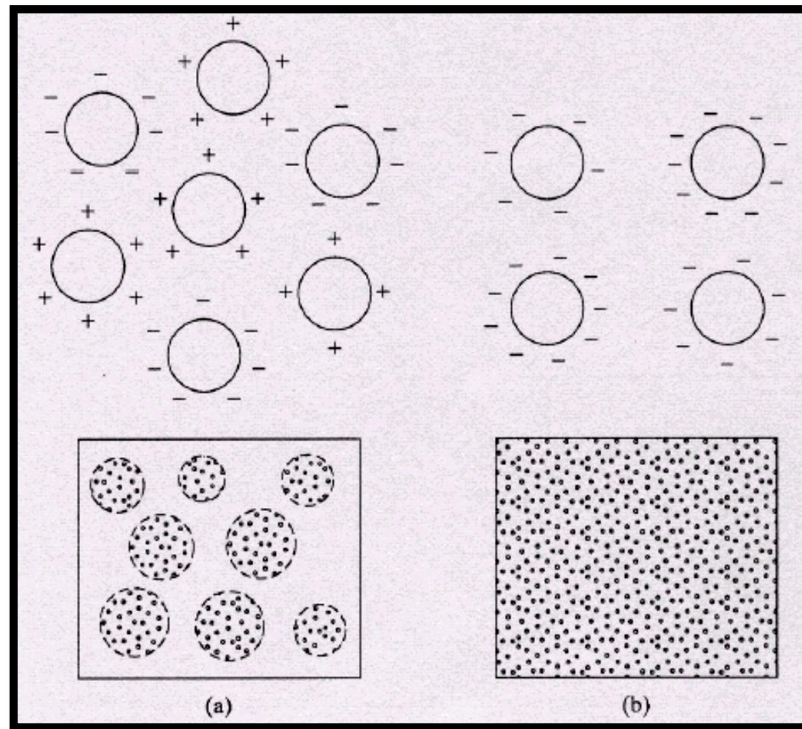


Figure 2.1 Dispersing action of water-reducing admixtures: (a) flocculated paste; (b) dispersed paste (Mindess et al., 2003)

2.4 Fly Ash

Fly ash is results from burning of coal in thermal power to produce electricity. Also called pulverized fuel ash. It is trapped by dust collection system inform of fine residue from burned gases and later released to the atmosphere. Meta-stable aluminosilicates are components of fly ash, its reaction with calcium ions in presence of moisture forms silica hydrates. Pulverization of coal used in thermal plants is vital before putting it to any use. The pulverization process begins with transporting of fine coal particles in an air stream to the boiler for combustion. Heat produced in combustion is used in the steam-generation unit to produce steam. During combustion, there is vaporization of volatile materials and burning out of carbon. Temperature increase of 1000-1500 degrees Celsius is recorded as particles enter the

burning zone. Coal gangue is the inorganic part of coal and contains minerals such as clays and feldspars. The minerals undergo melting process to form fused droplets that undergo solidification as spherical glassy particles when cooled. However, not all minerals undergo the process thus remain in the crystalline phase. At the end of the process, the coarser ash forms at the bottom of the furnace, and is referred to as the bottom ash. The transportation of fine ash is by flue gases and collection done by precipitators, the ash is therefore referred to as fly ash (Luke, 2002).

Fly ash is considered a common artificial pozzolan in the world. Application of fly ash in concrete technology began in 1930. A yearly estimation indicates a production of 450 million tons of fly ash worldwide. In the estimation, six percent used as pozzolan in concrete mixture culminates from the total fly ash (Mehta, 2000). There are twelve coal-burning power plants in Turkey producing about 15 million tons of fly ash yearly (Bayat, 1998 and Tokyay, 1998). Utilization of fly ash can be through blending component in the cement or separate additions in the concrete production. ASTM C618 (2008) categorizes fly ash into two mainly Class C and Class F. Class C fly ash contains analytical CaO of 15 percent to 35 percent while Class F contains less than 10 percent CaO (ASTM C618–2008). Additionally, Class F fly ash emerges from combustion bituminous and anthracite coals. It is characterized by low lime flash thus classified as pozzolan. Contrasting this, manufacture of Class C fly ash is from the combustion of subbituminous or lignite coal, it has pozzolanic and cementitious properties due to calcium properties (Naik et al., 1992). Figure 2.2 represents fly ash particles characterized by spherical, glassy particle shapes with different varying sizes from 1 μ m to 100 μ m (ACI Committee 232-1996).

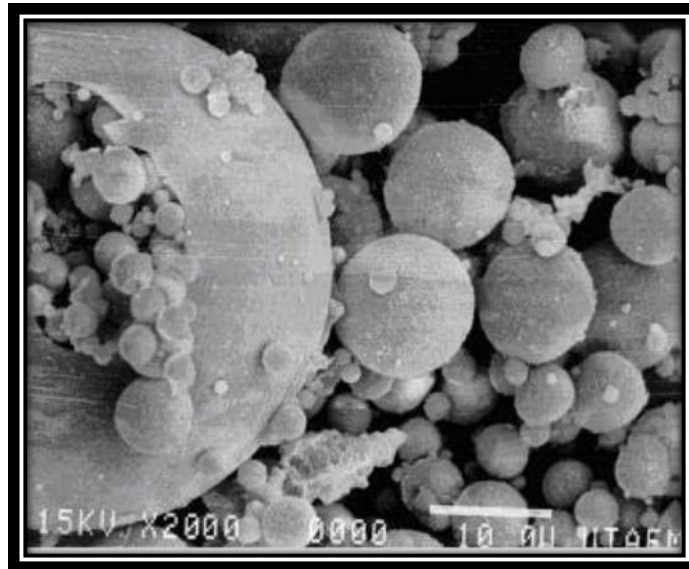


Figure 2.2 Fly ash particles (ACI Committee 232-1996)

2.5 Ground Granulated Blast-Furnace Slag (GGBFS)

GGBFS is a by-product in the production of iron. The components of iron ore are mixture of iron oxides, silica and alumina, various chemical reactions in the blast furnace results to reduction of iron ore to iron. The iron is then mixed with coke and limestone in the furnace. During the process, there is formation of a slag at a temperature of 1300 to 1600 degrees Celsius in form of liquid layer on top of liquid iron, which undergoes collection and cooling (Lee, 1974). The cooling process has various effects on the slag for instance when subjected to rapid cooling its structure is non crystalline and glassy. Notably, if water is involved in the cooling it is possible to retain sand sized particles of slag. During the granulation, there is necessity of using pelletization treatment. Thereafter the granular slag undergo drying and finally ground to finer cement. In the iron production process there is production of about 300 kg of slag for each ton of pig iron (Neville, 2004). However, the amount of slag obtained in older technology was high. Using blast furnace slag as

a cementitious material was a development in the second half of the nineteenth century. It is observed that 100 million tons of slag is produced yearly worldwide but with minimal utilization. Using an example of Europe, slag is mainly used as a component in blended cements but level of utilization varies depending with the country. For instance, Netherlands uses 90 percent of its slag produced (Regourd, 2004) and market share of slag is 60 percent (Bijen, 1996).

According to American slag association, in 2003 concrete and construction applications 3.1 million tons of slag used in the United States. The usage was in the blending of cement and addition in concrete production.

Blast furnace slag contains chemical composition nearly the same as Portland cement despite usage of pozzolanic by-products in blending. Notably, the composition of chemical in the slag relies on the cooling procedure and iron production materials. Slags contain CaO content of between 40 percent and 50 percent. In the classification of blast furnace slags, three respective grades are considered mainly: 80, 100 and 120. The classification is considered to the strength to the mortar that has 50 percent slag by volume. The size of the particle is determined from the grinding process (ASTM C989, 1999). The visible features of blast furnace slag particles are rough and sharp edged as illustrated in figure 2.3.

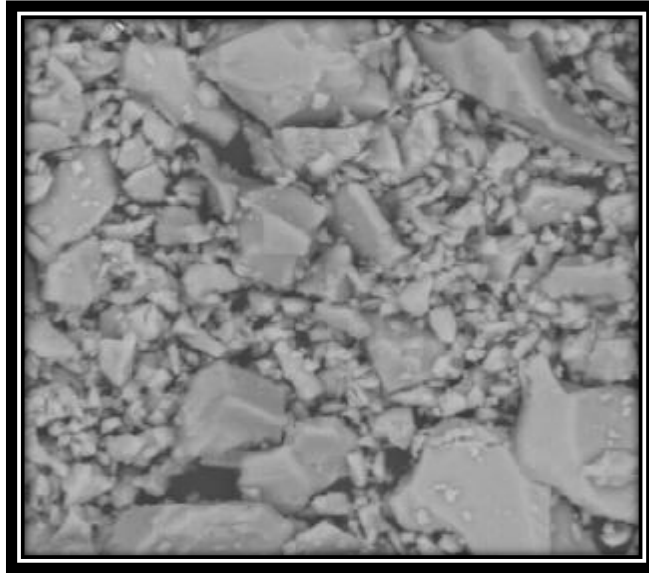


Figure 2.3 Ground granulated blast furnace slag particles (ASTM C 989, 1999).

2.6 Pelletizing Process

2.6.1 Definition

A. G. Anderson a Swedish researcher in 1912 came up with the idea of pelletization or agglomeration and C. A. Brackelsberg a Germany who also thought of the process. The process involves adding of binder to the fines agglomerated and strengthening of pellets at constant temperatures during production. The recommended size of the grain is attained through agglomeration or crushing. Pelletization is carried out by incitement that involves powder particles on an inclined rotating disk that contains a wetting agent and suitable binder. During the process there is balling of materials through creation of seeds that later grow into pellets of definite maximum size of about a diameter of 9.5 mm to 15.87mm (Bijen, 1986). The pelletization process is vital since it is used in the manufacture of coarse aggregate. For the efficacy in production of pellet, it is important to consider factors

such as pelletizer's disc revolution speed, moisture content, and pelletizer disk angle (Ramamurthy and Harikrishnan, 2006).

There are various types of pelletizer machines used in making of pellets; pan type, drum type, cone type and mixer type. Using disk type is advantageous as it is easier to control the drum type pelletizer. Contrastingly, mixer type pelletizer there is formation of grains with an increased particle size by the shape of the disk as illustrated in Figure 2.4 (Bijen, 1986). Pellets increase in relation to binder/cement ratio by weight of 0.2 onwards when cold bonded method is used (Yang and Huang, 1998). The effects of the disk angle and moisture content are on the parameter and they cause enlargement on the pellets (Ramamurthy and Harikrishnan, 2006). The binding agent dosage is vital in making of balls having an optimum range of 20 percent to 25 by total binders' weight (Bijen, 1986).

In the initial stage of the process, there is an addition of a certain percentage of water in the binder, which is later poured in the disk. The water remaining is sprayed during the rotation period, rotation without water leads to formation of lumps by fly ash and hence the distribution of particle size is stagnated. Formation of pellets takes duration of 20 min. The product produced at the end of the process is known as Fresh pellet. The fresh pellets should have high crushing strength to enhance transportation and stockpiling. The engineering performance increment rate, fine pellets and aim of use leads to pellets being sintered through time interval after production (Gesoglu, 2004; Doven, 1996; Jaroslav and Ruzickova, 1987; Pietsch, 1991).

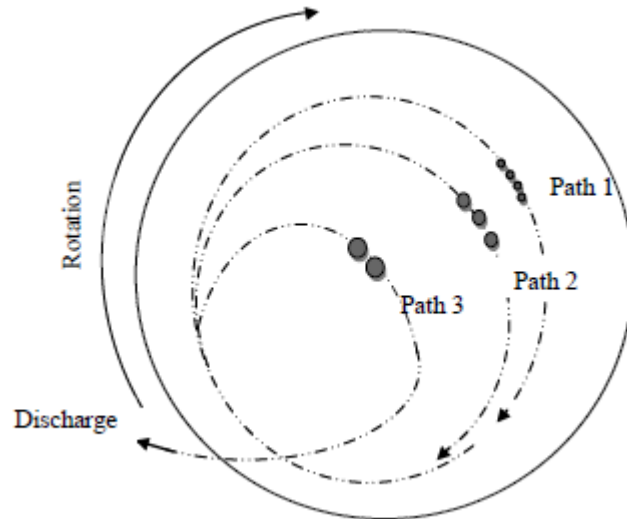


Figure 2.4 Growing path of pellets (Bijen, 1986).

2.6.2 Pelletization Mechanisms

Pelletization is a process of making nearly spherical pellets through tumbling of moist particulate fines by use of either additional binders or other needed additives such as drums, cones and discs. Many industries use pelletization in avoiding problems brought by fine particles. These industries are of; minerals, chemical, nuclear, fertilizer, pharmaceutical, waste processing, food and ceramic. Notably, the application of pelletization reflects in the concentrations of iron ore. There are different publications of practical and theoretical pelletization of fine particles comprising of detailed reviews (Goldstick, 1962; Kapur, 1978; Sastry and Fuerstenau, 1977). The tendency in the pelletization of fine particles lowers the amount of surface energy available in the total system by reducing the needed air water in interfacial area as shown in Figure 2.5 (Sastry and Fuerstenau, 1977). There are two respective forces that results in this change mainly physical and applied (Sastry and Fuerstenau, 1973).

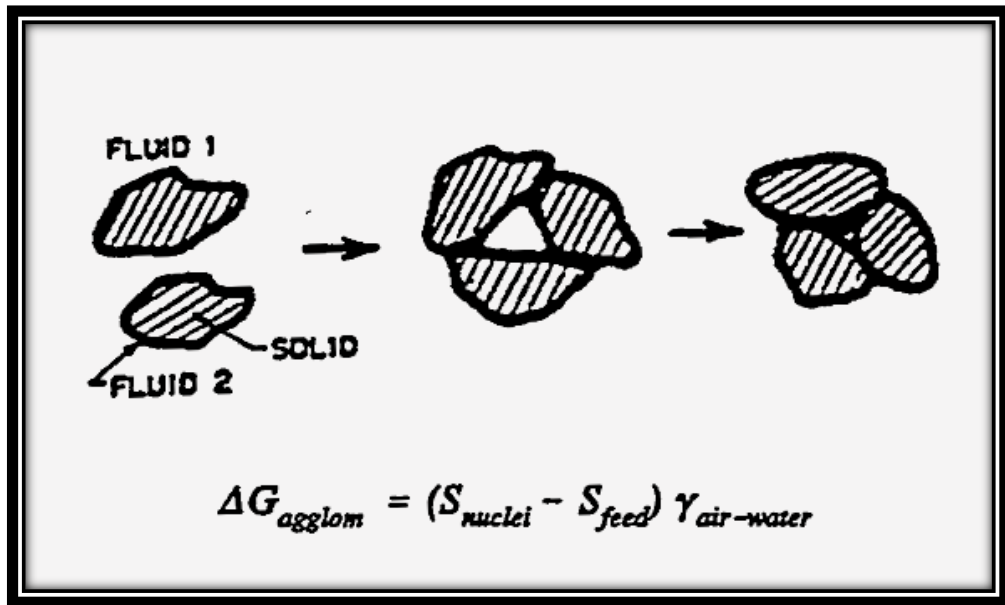


Figure 2.5. A schematic showing the driving force for pelletization due to reduction in total air-water interfacial area (Sastry and Fuerstenau, 1977)

Sources of physical forces for pellet formation and strength are; interfacial effects giving rise to capillary and surface tension forces, van der Waal's interaction, magnetic and electrostatic interactions, interlocking effects among particles and immovable bridging bonds. Applied forces arising from tumbling motion brings the wetted liquid particles into proximity with each other for physical forces to be operative thus enabling pelletization.

According to calculation by Rumpf (Rumpf, 1962) wetted solid particles by a bridging liquid, tension from the capillary and surface tension are predominant. The capillary magnitude forces rely on the existing bond type between the magnitudes. The bonds are classified depending on the relative proportion and air-water distribution phases in pellets. These forces include; pendular, funicular and capillary bonds. The three bonds are responsible for changes in the agglomerating system notably it is easier putting into use of size change mechanisms, which is accompanied with merit in cases of inadequate understanding of different forces at a

molecular level. There are seven mechanisms of agglomerate formation and size (Sastry and Fuerstenau, 1973). These are; dissociation, coalescence, breakage, layering, attrition, nucleation and abrasion transfer. Considerations of the three namely; nucleation, coalescence and layering are enough in our dialog (see Figure 2.6).

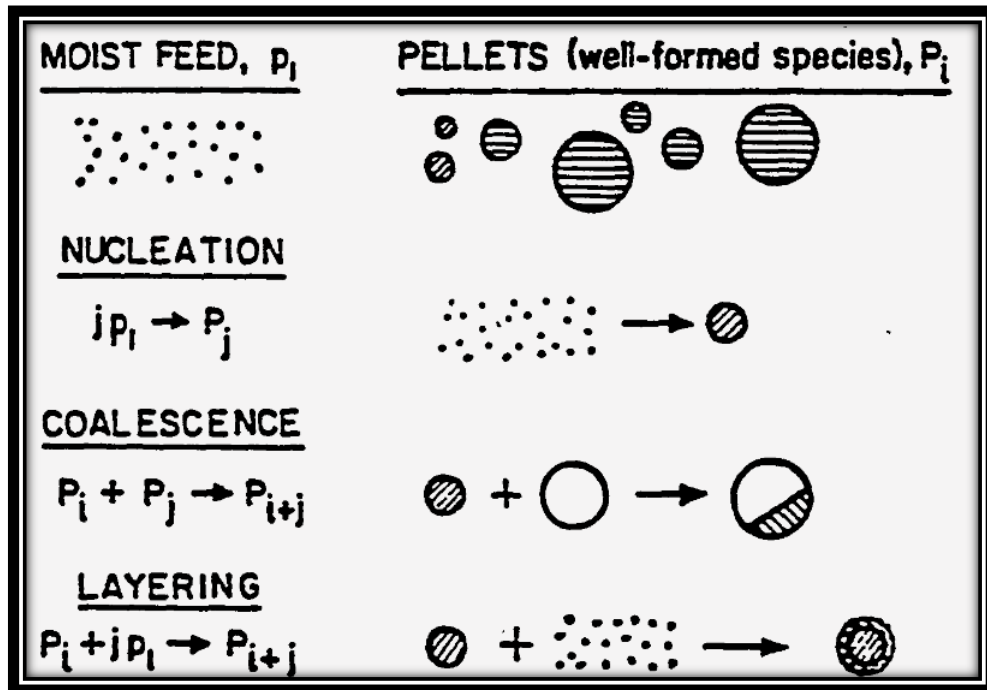


Figure 2.6. Three main mechanisms of pellet formation and growth: nucleation, coalescence, and layering (Sastry and Fuerstenau, 1977).

Nucleation is a process where particles are formed from the continuous phase because of interactions in the environment. The effect of nucleation is in formation of new particles with a discrete size of new agglomerates. Coalescence occurs immediately after the formation of nuclei. It is accompanied by change in the discrete size and decrease in the number of agglomerates. Layering mechanism also leads to the changing size of the particles due to interactions of particulates with the environment also known as continuous phase. Layering causes change in mass of the

agglomerates. Notably, the occurrence of layering depends on the presence of new agglomerates and new feed.

There is a continuous occurrence of the mechanisms in any agglomeration process unless there is selection of the design and operating conditions. However, the continuous occurrence results in undesirable size distribution of the agglomerates and cycling performance of the agglomerating unit. Additionally, the type of feed being pelletised can sustain growth mechanisms. Studies by Kapur and Fuerstenau shows that (Kapur and Fuerstenau, 1964), nucleation speeds the growth of pellets in the initial stage of batch pelletization then later coalescence mechanism is applied. There is a limited breakage of pellets in later stages. Layering mechanism is highly used in industrial pelletizing operations where moist feed is charged to the device continuously.

The estimation of water content is between 20 and 25 percent. Figure 2.7 illustrates ball formation mechanism less than the optimum moisture content. During the process, there is closer movement of particles in order to be connected with water bridges. Increase in the degree of saturation decreases the voids' volume thus driving out air and leaving the pore spaces for water and particles. Notably, capillary bonding occurs at this stage if feds are available in the additional moisture.

As illustrated in Figure 2.8, formation of ball is shown with optimum moisture content. In the ongoing ball formation, there is excessive wetting because of weak formation and lack of capillary force. The formation is characterized with random sizes that can easily be destroyed by mechanical forces in the balling drum and disc. Despite of the process is successful; a demerit occurs where there is lack of control to

granulometric distribution of pellets during pelletization process. The damage of the capillary force is felt below and above the optimum binder amount that later contributes to the engineering performance and size of the pellets produced.

The final better performance is initiated by maintaining the optimum moisture content equal to or below than the moisture content (Gesoglu, 2004; Doven, 1996; Jaroslav and Ruzickova, 1987; Pietsch, 1991).

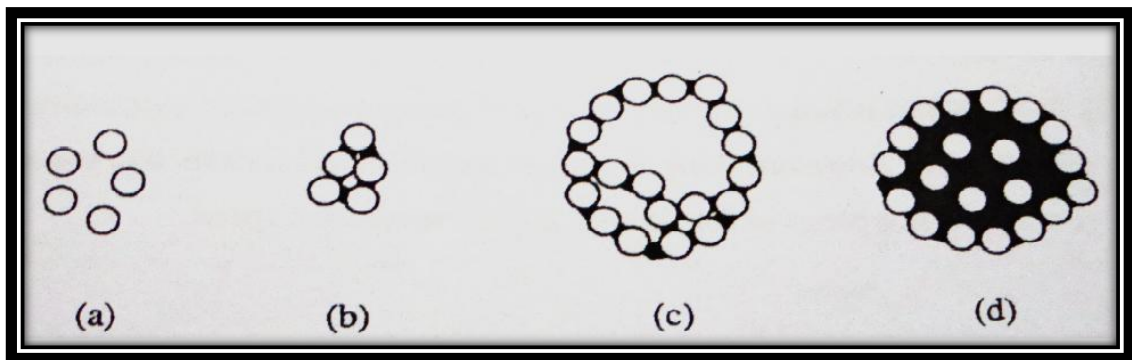


Figure 2.7 Nuclei ball formation mechanism (water content below optimum state)

(Doven, 1996)

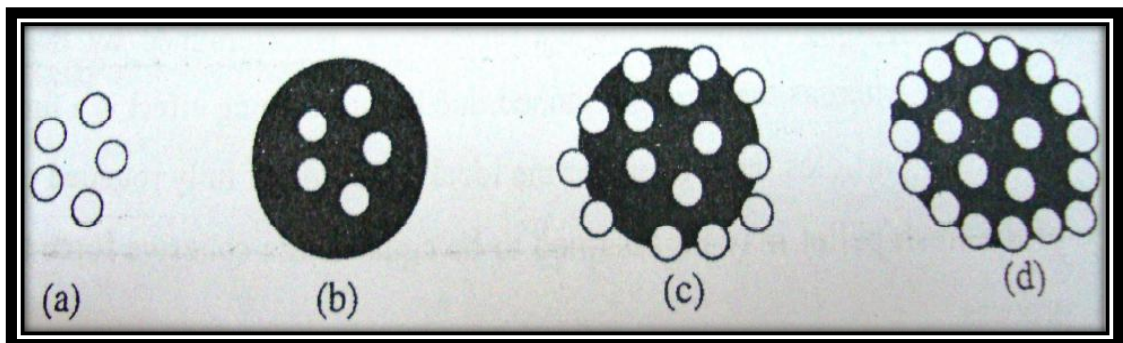


Figure 2.8 Nuclei ball formation mechanism (water content above optimum state)

(Doven, 1996)

2.7 Bonding between Cement Paste and Aggregate

The physical strength and reliability of the concrete mixture witnessed is due to the aggregate-cement paste interface, the bond is found on aggregate particles and near

hydrated cement. The cement paste and aggregate properties are used in enhancing the functionality of the interface (Dhir and Dyer, 1999).

The interfacial transition zone (ITZ) is a region surrounding the aggregate particles that differ from the bulk paste. There is variation in the cement aggregates in terms of shape, chances of holding dust, roughness of the surface and degrees of porosity (Barksdale, 1993).

Studies by Kosmatka et al on aggregate effect on high strength concrete put a priority of further consideration on the shape, size, surface texture, cleanness and mineralogy of the aggregate. Aggregate self-strength and its bond are vital factors in high strength concretes. Evidence from test results shows that compressive strength arising from use of crushed stone aggregates was higher than the gravel aggregate concrete in size and the cementing materials content.

There are other assumptions on using rough, angular and crushed materials, which results in the increase of strength because of the existing superior aggregate-paste bond (Kosmatka et al., 2002). Additionally, the aggregates applied in high strength concrete should be clean to prevent it from being attached to detrimental coating impurities of clay and dust as it has effect on fineness and quantity, water demand and aggregate –paste bond (Mindess et al., 2003).

Relying on previous studies, obtaining better parameters of concrete depends on suitable materials chosen and the adjustment of physical interfaces among the materials. There are different properties from bulk cement paste when 25-50 um thick zone surrounding the aggregate is considered, porous shell and a duplex layer of calcium hydroxide- $\text{Ca}(\text{OH})_2$. Notably, the considerations are responsible for promoting the accumulation of oriented calcium hydroxide crystals thus increasing

the weak planes where micro cracks occur. Various methods were suggested to help in improvement of the aggregate paste interface. These include decreasing the water ratio, including small amount of micro-silica and pre-coating the aggregate particles with the reactive layer of cement-micro silica slurry. All these causes increase in bond strength that can be observed in the compressive strength increase and elimination of the transition zone witnessed in porosity reduction (Subramanian, 1999). The presence of properties such as strength, aggregate-cement paste bond and permeability for water and ions come because of weak and porous composition of the interfacial transition composition (ITZ). Because of its 50um thickness and porosity, it holds a large amount of cement matrix hence affecting the aggregate and cement paste bonding. Investigation on the interfacial transition zone has overwhelming evidence that syneresis is an event that leads to formation of water rich layer around the aggregate weakening the aggregate-paste bond. Syneresis occurs when rapid flocculation is sustained by the system causing linkage between particles to two or three other particles, these results in a loose flock. The weak structure is characterized by considerable amount of entrapped water. There is contraction of the dispersal phase when a great number of contacts are created and decrease in its volume causes water ejection from the flocks (Bijen and de Rooij, 1999). Discoveries obtained in the same study shows the presence of fly ash and silica fumes in the concrete is because of the pozzolanic reaction mechanism therefore, there is need of decreasing the thickness in the interfacial transition zone.

From an inspection carried out by Detwiler et al on the firm orientation of calcium hydroxide crystals in the interfacial zone were examined in reference to the orientation of calcium hydroxide in the crystals. Additionally the same study found out that the axes of the crystal were vertical to the aggregate surface, and degree of

orientation increases with time without depending on the size and types of the aggregates (Detwiler et al., 1988). A study was carried out on the roll of the surface conditions of the aggregate on the compressive strength of concrete and aggregate-cement bond. In the study, there is utilization of 15mm of ground glass ball diameter together with different roughness degrees used as aggregate particles. From the results, increasing the degree of aggregate particles roughness reduces formation of micro cracks in the interfacial transition zone hence leading to development of the aggregate- cement bond and compressive strength of the cement. Besides the concrete strength made of elected aggregates depended on strength from aggregate particles-cement paste or cement paste (Perry and Gillott, 1977).

2.8 Shrinkage in Concrete

Definitions of shrinkage is based on two perspectives, (ACI-116, 2000) defines it as the decrease in length and volume in concrete. Another definition is simple contraction of concrete upon loss of water (Aïtcin et al., 1997). There are six types of shrinkage in these definitions namely: thermal shrinkage, plastic shrinkage, chemical shrinkage, autogenous shrinkage, drying shrinkage and carbonation shrinkage. Thermal is applicable and vital in the initial days after concrete placement, where heat produced due to cement hydration raises the concrete temperature. Concrete undergoes thermal shortening when subjected to cooling thus creating tensile stress in the concrete if there is no movement. There is a possibility of thermal shrinkage stress overcoming the low tensile strength of concrete at early age production hence causes cracking. Notably, autogenous and drying shrinkage are considered in add to thermal shrinkage.

2.8.1 Autogenous Shrinkage

Autogenous shrinkage depends on two factors namely: the concrete mixture design and the hydration process which are crucial properties of concrete. Autogenous shrinkage is small with values of 40 $\mu\epsilon$ at initial stages and 100 to 150 $\mu\epsilon$ in long term (Neville, 2004; Aïtcin et al., 1997; Carreira and R.G. Burg, 2000). The shrinkage tends to increase with increase in hydration rate hence cement containing higher C3A (tricalcium aluminate) content, finer cement, using supplementary cementing materials (SCMs), lower water-cement ratio and finer pore structure leads to increase in autogenous shrinkage.

Definitions and measure of autogenous shrinkage came up from Lynam in 1937 and Davis in 1940. Lynam came up with assumption that cause of autogenous shrinkage neither thermal effect and nor loss of moisture in the air. From Davis results, it was evident that after five years the autogenous shrinkage was in the 50-to-100 $\mu\epsilon$ range, which was smaller than the thermal and drying deformation at that time. Currently the paste has greatly changed due to use of high-range water reducers, higher cement contents, low water-to-cementitious material ratio and the use of SCMs (Jensen and Hansen, 2001). The increase in the autogenous shrinkage is accelerated by the change in microstructure in some instances becoming greater than the thermal and drying shrinkage. Carrying out comparisons between autogenous and drying shrinkage using concrete mixtures with water-to-cement ratio between 0.17 and 0.40 (Tazawa and S. Miyazawa, 1995), shows that the autogenous shrinkage of 0.40 water-to-cement ratio mixture at the initial stage was 100 $\mu\epsilon$ which is a representation of 40 percent of the total shrinkage (250 $\mu\epsilon$). Besides the autogenous shrinkage of the 0.17 water-to-cement ratio was previously 700 $\mu\epsilon$ representing 100

percent of the total shrinkage. Additionally, another study was carried out where it measured the autogenous shrinkage of 0.3 water-to-cementitious material ratio and cement paste in excess of $\mu\epsilon$ after two weeks (Jensen and P.F. Hansen, 2002). In cases where the cement has not developed fully in strength, the volumetric changes and thermal shrinkage results to cracking in concrete (Jensen and P.F. Hansen, 2001). There are various agreements that the chemical shrinkage is a reduction in volume caused by hydration thus does not show macroscopic changes after the final setting. Besides, the autogenous shrinkage is a result of self-desiccation hence it shows after the final stage.

According to Le Chatelier in 1900, volume formed during hydration of Portland cement is less than the total water and cement. Notably, the Le Chatelier's phenomena contraction is the possible cause of chemical shrinkage. The volumetric contraction is between 8 and 12 percent (de Larrard et al., 1994). These contractions involve free movement of cement paste before reaching the final set. The movement helps in accommodating the change in volume. The rigid skeleton is useful at the final stage in preventing more contractions hence creating pores and increasing their size. Following further cement reactions, there is tendency in increase of water used in the reaction, dropping of relative concrete humidity thus leading to creation of capillary stress that causes shrinkage in concrete. The shrinkage that results from the stress is known as autogenous shrinkage (Jensen and P.F. Hansen, 2001).

2.8.2 Drying Shrinkage

Drying shrinkage is contraction brought about by moisture migration in the concrete (ACI Committee 209, 1997). In this type of shrinkage, water is not used in cement

reaction instead; it is lost in the environment thus that differentiates it from autogenous shrinkage.

Drying shrinkage mainly depends on external characteristics such as member size, shape and environment thus making it not to be a constitutive property of concrete. There is one major driving force of drying shrinkage, which entails removing absorbed water from hydrated cement (Mehta and P.J.M. Monteiro, 1993). Additionally the continuous removal of water in the small capillaries culminates to shrinkage through tensile hydrostatic forces (Aïtcin et al., 1997). It is difficult for absorption of water when it is strongly tightened to the hydrated cement paste. Seemingly, with time there is a decrease in water loss rate as demonstrated in Figure 2.9. The (CEB-FIP-2001) came up with values to show the final drying shrinkage under a relative humidity of 50 percent for a 24.1 MPa (3500-psi) concrete of 645 $\mu\epsilon$. Under standard ambient conditions (23 C⁰) in the conventional concrete with percentage of 50 relative humidity, drying shrinkage in 75 to 150 mm-deep specimens ranging between 400 and 800 $\mu\epsilon$ after two years. Time is an influential factor in the drying shrinkage. Increase in time results to more water being drawn from capillaries thus resulting to larger shrinkage. There is disagreement on the importance of the drying age. The commonly used empirical models in the estimation of considered time in drying shrinkage using drying as a variable but only two used age at the beginning of drying (ACI Committee 209, 1997; CEB-FIP 1990; AASHTO, 2004; Bažant and S. Baweja, 1995; Gardner and M.J. Lockman, 2001; Sakata, 1993; Sakata et al., 2001).

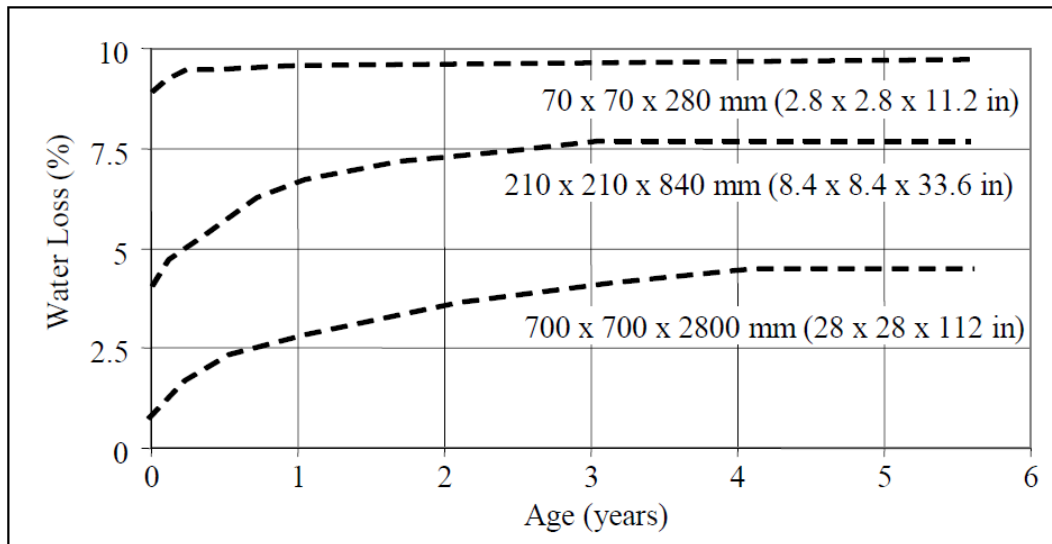


Figure 2.9: Water loss versus time from concrete specimens of various sizes under 55% relative humidity (Aïtcin et al., 1997)

2.9 Mechanisms of Shrinkage

Three respective mechanisms give an explanation to the shrinkage of cement paste during the drying process. These mechanisms include; change in volume by capillary stresses, by disjoining pressure and by surface energy. They are related to the water migration in cement paste, the volume change of drying concrete is not the same because of differences in the tightness of water bound to the microstructure as illustrated in Figure 2.10.

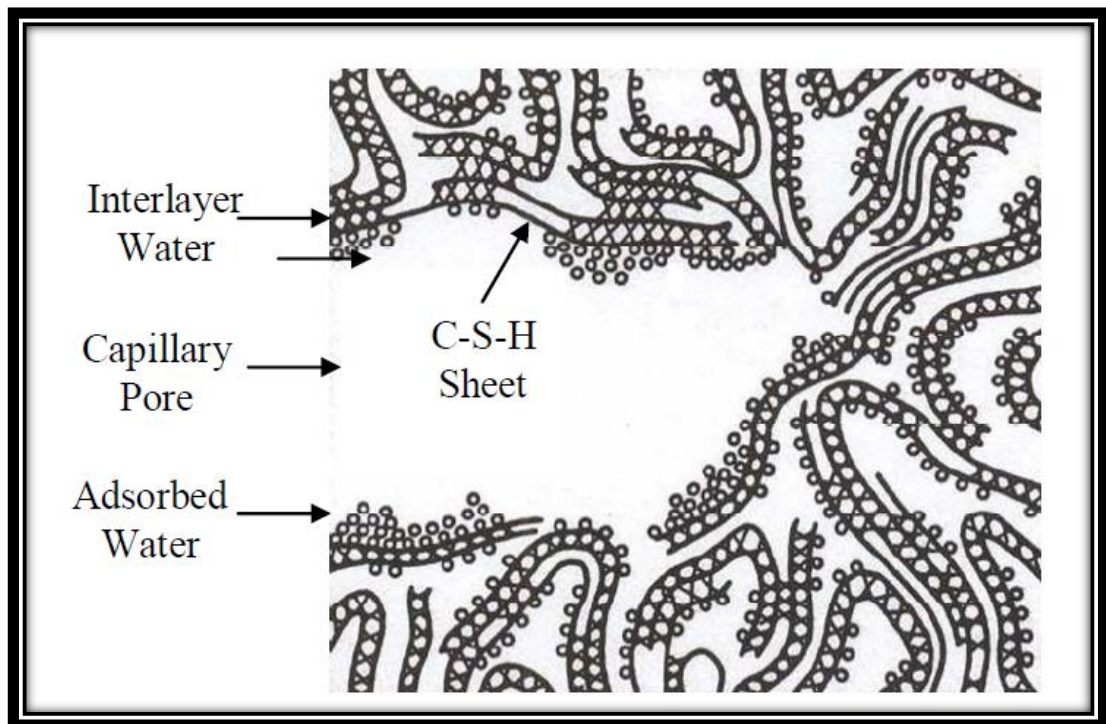


Figure 2.10: Representation of cement paste microstructure (Mehta and P.J.M. Monteiro, 1993)

Initially there is presence of capillary water that is easier to move. However, the force required for water removal from the capillaries is inversely proportional to the size of the capillary. Water is therefore withdrawn from the void space in large pores followed by smaller pores.

Secondly, it is difficult to remove absorbed water bound to the present surface area in C-S-H, capillary pores walls and other hydration products such as ettringite.

Thirdly, there is presence of interlayer water that is bound to two or more C-S-H sheets. This water is more complicated to remove as it is linked to two or more C-S-H surfaces and it contains one layer of molecule of water molecules (Mehta and P.J.M. Monteiro, 1993). Lastly, there is the chemical bonded water that found in any hydration product, not shown in Figure 2.3 .Production of this water depends on high

temperatures where there is decomposition of hydration products. Agreements from researchers are on three drying mechanisms, which are related to forces brought about by migration of water in the capillary pores, absorbed water and chemically bounded water. These mechanisms include; Capillary Stress that occurs when water is removed from the capillary pores resulting to stress. There is creation of a new liquid-gas when the water in the pores are removed, the process requires more energy leading to the creation of a curved surface in the pore walls with an aim of minimizing the interface energy in water gas. This causes tension stress in the capillary and therefore subjecting the walls of the pore to compression (Mindess et al., 2003; Wittmann, 1982). The pore size has effects on the amount of shrinkage, for instance the smaller the pore the higher the capillary stress. Shrinkage emerging at this point arises from hydrostatic tension in the small capillaries (Mindess et al., 2003; Neville, 2004; RILEM TC69 Subcommittee 1, 1988). Because of water removal in the capillaries, there is little or no shrinkage.

Disjoining pressure is the second mechanism, RILEM TC69 (RILEM TC69 Subcommittee 1, 1988) powers in 1965 was first in noticing that below 40 percent of humidity shrinkage was higher than the predictions from the capillary stress theory thus made conclusions that there was another mechanism causing shrinkage. Notably, low humidity results to removal of water in the capillaries thus resulting to loss of absorbed water by C-S-H as demonstrated in Figure 2.3. Depending on the relative humidity, absorbed water can contain many layers of water. Decrease in the relative humidity results to decrease in thickness of the absorbed water layer hence causing reduction to the disjoining pressure Munich model (Wittmann, 1982). This

stage is accompanied with change in volume of unrestrained cement paste to volume of water removed.

Finally, there is the surface energy, which is brought about by the disappearance of pressure as a reduction of relative humidity below 50 percent. During the most of the absorbed water has been removed thus increase in the surface free energy of the C-S-H resulting in contraction. Additionally, proposal by Bangham and Fakhoury in 1931 (Wittmann, 1982) identify the existence of a linear relationship between change in surface energy and change in length.

2.10 Internal Curing Overview

Internal curing entails placing of water in an encapsulated state within the concrete to be used in hydration of the cement matrix (Henkensiefken et al., 2011). Water encapsulation occurs in many ways and then batched directly into the concrete mixture itself. ACI (2010) makes a description of internal curing as supply of water in a cementitious mixture by use of reservoirs through pre-wetted lightweight aggregates that releases water needed for hydration and replacing the evaporated moisture (Bentz and Weiss, 2011). The reservoirs are not limited to superabsorbent polymers, lightweight expanded clay and shale aggregates (LWA), Bentonite clays and the natural material such as pumice (Jensen and Lura, 2006). The internal curing material mainly pre soaked in water. Encapsulation of the additional water the ratio of water to cement (w/c) is unaffected. The water is termed as additional and utilized during hydration (Bentz et al., 2005). The water from external curing is same as that added from internal curing. Water added from external curing for instance shocked plastic sheeting and wet burlap is not added to the water cement ratio of traditional

mix design. More so water absorbed by LWA is not considered in the w/c of internally cures concrete (Roberts, 2006). In internal curing water is distributed consistently, during curing thus hydration of interfacial zones (ITZ) around the aggregate particles (Henkensiefken et al., 2009). Figure 2.11 shows a graphical representation between external and internal curing. There is desorption of water in the LWA as result of internal suction stress generated when cement particles undergoing hydration as the hydrated cement particles become devoid of water available. (Bentz and Snyder, 1999). The availability of suction pressure allows desorption of water from LWA as needed in hydration as described by (ACI, 2012). Water from LWA causes decrease in the internal pressure buildup caused because of hydrating cement particles becoming devoid of the necessary water (Holt, 2001). The negative effects that occur during hydration of low w/c are avoided by providing necessary water for hydration purposes (Bentz and weiss, 2011).

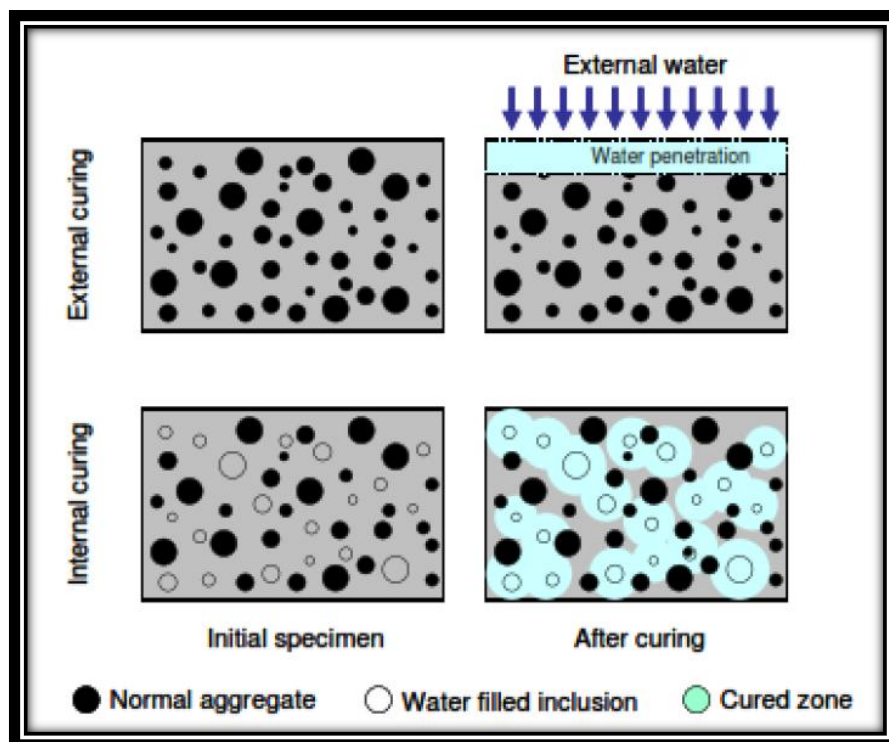


Figure 2.11 LWA moisture transfer to hydrating cement paste (Castro et al., 2010).

2.11 Method to Incorporate Water in Concrete

(Philleo, 1991) was the first to come up with suggestions on internal curing by use of lightweight aggregate in 1991 (Bentz and K.A. Snyder, 1999). There are various investigations on using lightweight aggregate as an internal curing reservoir (Bentz and K.A. Snyder, 1999; Weber and H.W. Reinhardt, 1997; Lura et al., 2003; Holm et al., 2003; Bentur et al., 2001; Hoff, 2003; Kohno et al., 1999; Zhutovsky et al., 2002; Hammer et al., 2002). The authors made exploration on usage of natural and lightweight aggregate, fine and course lightweight aggregate and the total replacement of normal weight aggregate by lightweight aggregate. Notably, the carried out demonstrations about the effectiveness of internal curing by use of lightweight aggregates have been effective. Lightweight aggregates can absorb 5 to 25 percent of percent after 24 hours of immersion; this is because of their porous structure (Holm and T.W. Bremner, 2000). The amount of lightweight aggregate in the mixture determines the amount of internally incorporated water. It can reach 59 kg of water per cubic meter of concrete (Holm et al., 2003), but the increase in kilograms can go up to 90 kg of water per cubic meter of concrete (Jensen and P. Lura, 2003). Conclusions finalize that there is spontaneous movement of water to lower energy levels (Jensen and P. Lura, 2003) for instance from larger to small pores, available pores in aggregate smaller than 0.1 μm have no contribution to internal curing. Additionally, it was also suggested that there are different lightweight aggregates and this efficiency in the internal curing depends on the structure of the pore (Hammer et al., 2002). Results indicate that the course pore structure is due to the expanded clay lightweight aggregates. This results to loss of most of its water at 97.4% relative humidity. Notably, expanded slate holds water down to 70 percent relative of humidity. From this, it is evident that the fine pore

structure of the expanded slate is less efficient for internal curing thus most of its contents are used in the achievement of internal curing than that of the expanded clay.

Transfer of water from pumice to the cement occurs during the first 24 hours (Cano Barrita et al., 2002). Additionally, 50 percent of water remaining in aggregate is not used in hydration. This is only practical when the pumice used has two well defined pore sizes. The pores include a large that gave up water easily and a fine pore that maintained its water. It is disadvantageous to replace normal weight aggregate by lightweight aggregate because it causes reduction in compressive strength and modulus of elasticity in the concrete (Aitcin, 1998; Holm and T.W. Bremner, 2000; ACI Committee 213, 2003). A more convenient and efficient use of Superabsorbent polymers (SAP) in incorporating water in concrete (Jensen and P.F. Hansen, 2002; Jensen and P.F. Hansen, 2001; Kovler and O.M. Jensen, 2005). There are different types of SAP with some that can absorb up to 5000 times of their weight in water. Most of them have absorption capacities of 50 times of their weight, which are used by the diaper industry and readily available. The polymers are added to the mixture as dry powder. In dry condition the polymers have an average size of 0.1 and 0.25 mm (0.004 and 0.01) which has a tendency of increment of up to three times in saturated condition (Jensen O.M. and P.F. Hansen, 2002). A porosity similar to that of entrainment agent is left after the SAP has given up water to the paste. Using polymers is advantageous compared to lightweight aggregate because much absorption allows reduction in the dosage to incorporate the same total water. Segregation of SAP may occur due to the low density it holds in comparison to other constituents (Jensen O.M. and P.F. Hansen, 2002). Increase in the effective water-to-

cement ratio is another demerit of using SAP in cases where their absorption capacity is diminished by other constituents. This may be a contributing factor to the 19 percent decrease from some mixtures with SAP (Jensen O.M. and P.F. Hansen, 2002). A comparison carried out on the effectiveness of internal curing with use of fine lightweight aggregate and SAP (Geiker et al., 2002) indicates that from the particular proportions, 20 percent of the fine aggregate is lightweight and 0.04 percent is the cement weight for SAP, all these produced adequate internal curing.

CHAPTER 3

EXPERIMENTAL PROGRAM AND METHODOLOGY

3.1. Introduction

Investigations were carried out on internal curing (IN) of high strength concrete made from artificial cold bonded fly ash aggregate (AFA) and artificial slag aggregates (ASA) through experimental programs with two parts. AFA and ASA were produced first through pelletization process of FA, GGBFS and cement at ambient temperature. Following their production AFA and ASA are used for high strength concrete production. Fresh unit weight with the slump test are meant to help in achieving the expected slump (150 ± 20) mm of handling, placing and consolidating in all concrete mixtures. Superplasticizer adjusted during mixing helps in achieving the specified slump. Various tests were carried out on the hardened concrete to determine the compressive strength and splitting tensile strength at 28 days and evaluation of mechanical properties. Additionally, the tests for physical properties were conducted for drying shrinkage, autogenous shrinkage, restrained shrinkage and weight loss.

3.2. Materials

3.2.1. Cement

In the study there was use of ordinary Portland cement (PC CEM, I 42.5R) conforming to TS EN 197-1 (Turkish Standard TS EN 197-1, 2002). The cement had 3.15 g/cm^3 of specific gravity and $326 \text{ m}^2/\text{kg}$ of Blaine fineness. Its utilization was based on the production of artificial aggregates and concretes. Table 3.1 shows the physical and chemical properties of cement.

Table 3.1 Physical and chemical properties of Cement, Fly Ash and Slag.

Chemical analysis (%)	Cement	GGBFS	FA
CaO	62.12	34.12	4.24
SiO ₂	19.69	36.41	56.2
Al ₂ O ₃	5.16	10.39	20.17
Fe ₂ O ₃	2.88	0.69	6.69
MgO	1.17	10.26	1.92
SO ₃	2.63	-	0.49
K ₂ O	-	0.97	1.89
Na ₂ O	0.17	0.35	0.58
Cr ₂ O ₃	0.88	-	-
Loss on ignition	0.87	1.64	1.78
Specific gravity	3.15	2.79	2.25
Blaine Fineness(m^2/kg)	394	418	287

3.2.2. Fly Ash

Fly ash (FA) class F according to ASTM C618 (ASTM C618-08, 2000) was supplied mainly from Ceyhan Sugoza thermal power plant. It had a specific gravity of 2.25 g/cm^3 and $287 \text{ m}^2/\text{kg}$ of Blaine fineness. The physical and chemical properties of fly ash are provided in Table 3.1.

3.2.3. Ground Granulated Blast Furnace Slag

Ground granulated blast furnace slag (GGBFS) was used in the manufacture of ASA and was obtained from Iskenderun cement production factory with a specific gravity of 2.79 and Blaine fineness of 418 m²/kg. The physical and chemical composition of GGBFS is also provided in Table 3.1.

3.2.4. Superplasticizer

To achieve target workability a superplasticizer (SP) with a specific gravity of 1.07 g /cm³ was used. Its properties are given in Table 3.2

Table 3.2 Properties of superplasticizer

Properties	High range water reducer admixture
Commercial name	Glenium 51
Color tone	Dark brown
State	Liquid
Specific gravity	1.07
Chemical description	Polycarboxylic-ether

3.2.5. Aggregates

3.2.5.1. Artificial Cold-Bonded Aggregates

AFA and ASA produced through a cold bonding process were used in manufacturing of HSC. During cold bonding, there is pelletization of a dry mixture of Fly ash/Cement and GGBFS/Cement with 10 percent weight proportions, through moisturizing in a rotating inclined pan at an ambient temperature. The diameter and

depth of the pelletizer pan used is 80 cm and 35 cm, respectively as illustrated in Figure 3.1.

To begin, a certain percentage of water was added to the mixture and then poured in the disk, the amount of remaining water is sprayed during the rotating period because rotation without water leads to formation of lumps by the fly ash or GGBFS and the causing no increase in the distribution particle size. The amount of sprayed water makes 18-20 percent by weight of the dry powder mixture, with formation of pellets in duration of 10 minutes. The second step continues with pelletization after formation, this is aimed at stiffening of fresh pellets and takes approximately 10 minutes. This makes the production to take about 20 minutes. The produced fresh pellets are thereafter placed in sealed plastic bags and stored for hardening in a curing room of 20 C^o and a relative humidity of 70 percent for 28 days. (Ke et al., 2009; Gesoğlu et al., 2012). Figure 3.2 shows self-curing process of the agglomerates and hardened lightweight aggregates.

The hardened fly ash and slag aggregates produced are then undergo separate sieving in to size fraction of 4-16 mm as lightweight coarse aggregate. There is need of determining the aggregate properties, thus specific gravity and the water absorption tests were conducted as per (ASTM C127, 2007), whereas the crushing strength test was carried out as per (BS 812, part 110, 1990). The measurement of the crushing strength was carried out by a dial gage and transformed to load. A sketch of the crushing strength apparatus is given in Figure 3.3. Failure of agglomerates results to the application of statistical force and there is a definition of statistical representation as the crushing strength or the crushing value.

To get the crushing strength, it is vital to consider the following Equation 3.1

$$\sigma = \frac{2.8P_{max}}{\pi x^2} \quad (3.1)$$

In this case, X represents the distance between loading points and p_{max} represents the fracture load (Yashima et al., 1987; Li et al., 2000; Mangialardi, 2001; Cheeseman et al., 2005). Water absorption of the coarse aggregate for AFA after 24 hrs of soaking in water was 20.81% while the specific gravity was 1.77, respectively. While, water absorption and specific gravity for ASA after 24 hrs of soaking in water was 7.47 % and 2.28, respectively. Moreover, crushing strength of the produced AA is shown in Figure 3.4. Additionally, sieve analysis and specific gravity of AA are shown in Table 3.3

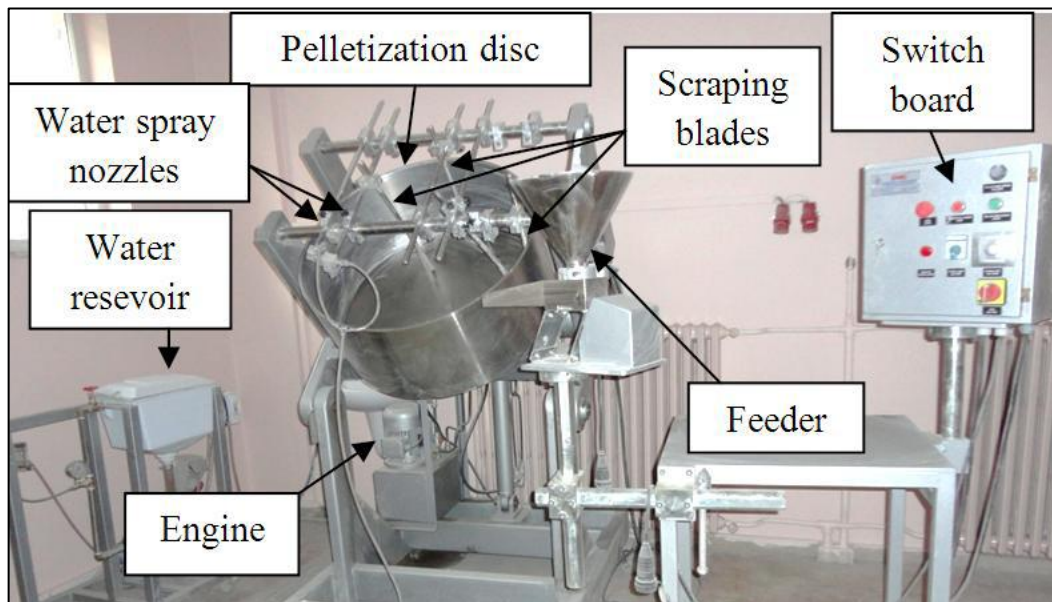


Figure 3.1 The general view of the pelletization disc



Figure 3.2 Artificial aggregate self-curing process



Figure 3.3 Crushing strength test apparatus

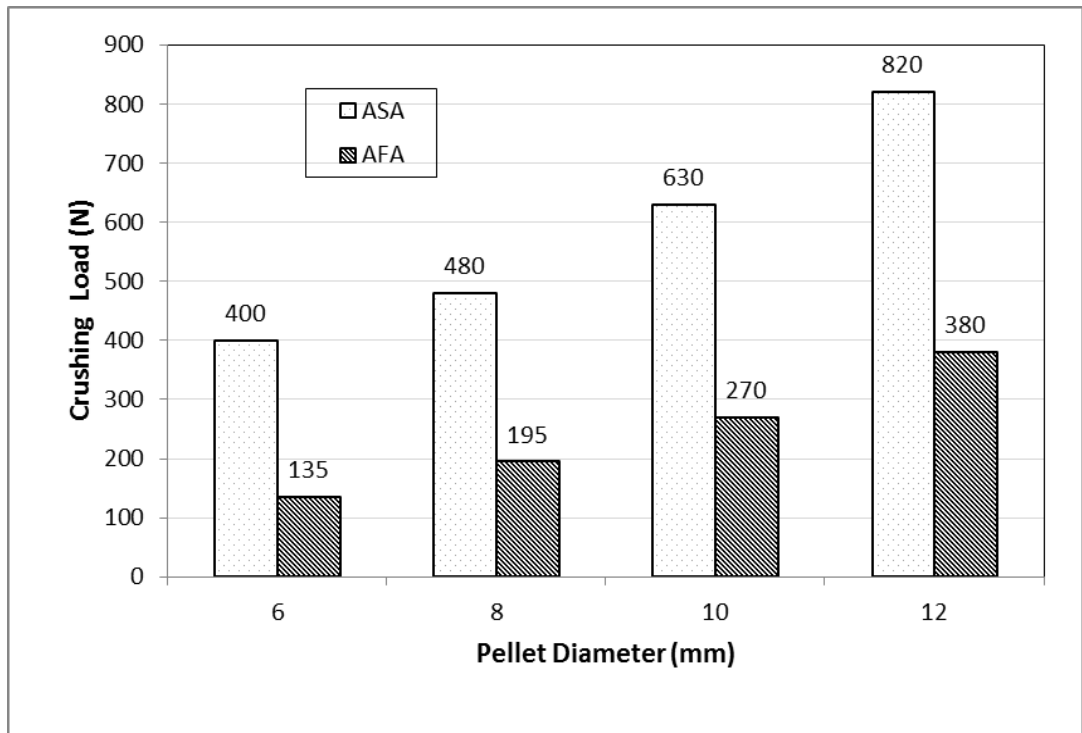


Figure 3.4 Crushing load of the produced artificial aggregates

3.2.5.2. Natural Aggregates

River gravel was used having a normal maximum size of 16 mm. In the fine aggregate natural sand river was used with a maximum of 4 mm. The fineness modulus and water absorption of the coarse aggregate was 5.61 and 0.45 percent, respectively. The water absorption in natural river sand was 0.66 percent. Table 3.3 shows the physical properties and the size distribution of natural aggregates and AA.

Table 3.3 Sieve analysis and physical properties of natural as well as artificial aggregates

Sieve size (mm)	Natural aggregate (%)		Artificial coarse aggregates (%)	
	NFA	NCA	AFA	ASA
16	100	100	100	100
8	100	35	28.1	44.662
4	100	0.44	0	0
2	56.8	0	0	0
1	35	0	0	0
0.5	22.7	0	0	0
0.25	16.4	0	0	0
Specific gravity	2.59	2.71	1.76	2.27

3.3. Concrete Mixture Details

To carry out investigations on the effect of cold bonded lightweight fly ash and slag aggregates on internal curing of high strength concrete, there is use of nine concrete mixtures at a water-cement ratio of 0.28. Besides, there is use of 570 kg/m³ cement content in all mixtures. The relevant testing parameters in cold bonded fly ash and slag aggregate are the coarse aggregate volume fraction. The volumes of LWCA used are 0, 5, 10, 15 and 20 percent of the total coarse aggregate by as illustrated in Table 3.4. Hence, the concrete mixtures were divided into two groups mainly FA aggregate and GGBFS aggregate. There is AFA0ASA0, which was used as a control mix having zero replacement of natural aggregates by lightweight aggregates. Hence, AFA5ASA0 to AFA20ASA0 that mixes with 5 to 20% AFA besides 0% slag, respectively. There is also AFA0ASA5 to AFA0ASA20 that mixes with 0% AFA and 5 to 20% ASA, respectively.

Additionally, the mixture proportions of SP are used in varying amounts to needed workability for all mixtures as presented in Table 3.5.

Table 3.4 Aggregates volume fractions for artificial coarse aggregates

Mix Code	(NFA) (%)	(NCA) (%)	(AFA) (%)	(ASA) (%)
AFA0ASA0	100	100	0	0
AFA5ASA0	100	95	5	0
AFA10ASA0	100	90	10	0
AFA15ASA0	100	85	15	0
AFA20ASA0	100	80	20	0
AFA0ASA5	100	95	0	5
AFA0ASA10	100	90	0	10
AFA0ASA15	100	85	0	15
AFA0ASA20	100	80	0	20

Table 3.5 Concrete mix proportions in kg/m³

Code	w/c	Cement	Water	Coarse aggregate			Fine aggregate	SP
				NCA	AFA	ASA	NFA	
AFA0ASA0	0.28	570.00	159.60	880.00	0.00	0.00	841.36	4.928
AFA5ASA0	0.28	570.00	159.60	792.00	57.35	0.00	841.36	4.800
AFA10ASA0	0.28	570.00	159.60	704.00	114.69	0.00	841.36	4.659
AFA15ASA0	0.28	570.00	159.60	616.00	172.04	0.00	841.36	4.480
AFA20ASA0	0.28	570.00	159.60	528.00	229.38	0.00	841.36	4.360
AFA0ASA5	0.28	570.00	159.60	792.00	0.00	73.91	841.36	4.672
AFA0ASA10	0.28	570.00	159.60	704.00	0.00	147.81	841.36	4.512
AFA0ASA15	0.28	570.00	159.60	616.00	0.00	221.72	841.36	4.340
AFA0ASA20	0.28	570.00	159.60	528.00	0.00	295.63	841.36	4.272

3.4 Concrete Casting and Curing

The casting in all mixtures was done by power-driven revolving pan mixer having a capacity of 30 liters using the special procedure for batching and mixing. In the procedure, there is use of bonded artificial lightweight FA and GGBFS aggregates as course aggregates in all concrete mixtures except control mix. There is immersion of LWA in water for 30 minutes for saturation before each mixing. Following this is the removal of LWA from water and placing it on mesh for the outflow of immoderate surface water for around 30 seconds. There after there was use of a dry towel in rubbing the extra water on pellets surface (Figure 3.5). It is effective to obtain SSD condition for artificial lightweight aggregates using this way (Gesoglu, 2004; Joseph and Ramamurthy, 2009; Gesoglu et.al. 2012). Initially, cement was mixed with LWA in SSD then course and fine aggregates were added to the mixer. After homogenization of the aggregates and cement for 30 seconds mixing, one third of mixing water was added to the mix for one additional minute. Finally, there was addition of SP and the remaining water in the mixing for 3 minutes and then the mix was left to rest for 2 minutes. Lastly, 2 minutes added to the mixing adapted thus completing the mixing sequence. The slump range of 150 ± 20 mm for high strength concrete was designed hence there was a continuous production of trial batches for each mixture until the desired slump was obtained through adjustment of SP. After the completion of the casting process, there was pouring of concrete into the molds in two and three layers with vibration for 30 seconds.

Specimens cast from each mixture consisted of the following:

- Six 150 mm *150 mm *150 mm cubes for the compressive strength and modulus of elasticity evaluation at 28 days.
- Three 100x200 mm cylinders for splitting tensile strength at 28 days.
- Three 70x70x280 mm prisms for drying shrinkage and weight loss evaluation.
- Three 70x70x280 mm prisms, for evaluation of autogenous shrinkage.
- Two ring-shaped specimens to display restrained shrinkage cracking.

To enhance autogenous deformation test specimens were placed in two layers of plastic sheets and placed in molds before pouring (Figure 3.6). After de-molding, there is sealing of each specimen using two layers of plastic sheets and two layers of aluminum foil (Figure 3.7). Notably, various measurements were taken in casting room at $20\pm 2\text{ C}^0$ and 65 percent RH, in regard to drying and restrained shrinkage test immediately after casting, thereafter there was curing of specimen for 24 hours in a cabinet with 100 percent relative humidity and a temperature of 20 C^0 for 28 days. Additionally, after the curing period, the removal of the outer mould of the ring led to covering at the top surface of the concrete ring by a silicon rubber to enable drying by the outer circumferential surface. Later there was de-molding of the free shrinkage test prisms. After fixing the gage length on each specimen using the glued pins on the prism face, there was recording of initial weight to enhance monitoring weight lost in the drying period. Then, there was subjection of rings and prisms specimens at $23\pm 2\text{ C}^0$ and 50 ± 5 percent relative humidity for around 60 days. After de-molding of all other specimens, there was curing by water up to testing age (Figure 3.8).



Figure 3.5 AAs in SSD condition



Figure 3.6 Plastic sheets inside the mold before the casting



Figure 3.7.a-) Specimens sealed with two layers of plastic sheets. b-) After plastic sheets specimens sealed with a layer of aluminum foil



Figure 3.8 The specimens in curing by water

3.5. Tests for Mechanical Properties

3.5.1. Compressive Strength

Compression test on cube specimens was conducted (150x150x150 mm) by a 2000 KN capacity testing machine in relation to (BS 1881-116, 2003) as illustrated in Figure 3.9.



Figure 3.9 Compressive strength test machine

3.5.2 Modulus of elasticity

Static modulus of elasticity was determined by the testing of cubes with a dimension of 150x150 x150 mm according to BSI 1881-121 (BS 1881-121, 1983). Each of the specimens was fitted with a compressometer containing a dial gage capable of measuring deformation to 0.002 mm (Figure 3.10) and then loaded three times to 40% of the ultimate load determined based on the compressive strength test results for each mix. The first set of readings of each cube was ignored and the modulus was reported as the

average of the second two sets of readings. For each parameter, three specimens were used.



Figure 3.10 Measuring modulus of elasticity

3.5.3 Splitting Tensile Strength

The tensile strength is determined in accordance with (ASTM C 496, 2012) on three $\Phi 100 \times 200$ mm cylinder for each mixture tested in 28 days. The tensile strength was calculated using the equation in 3.3.

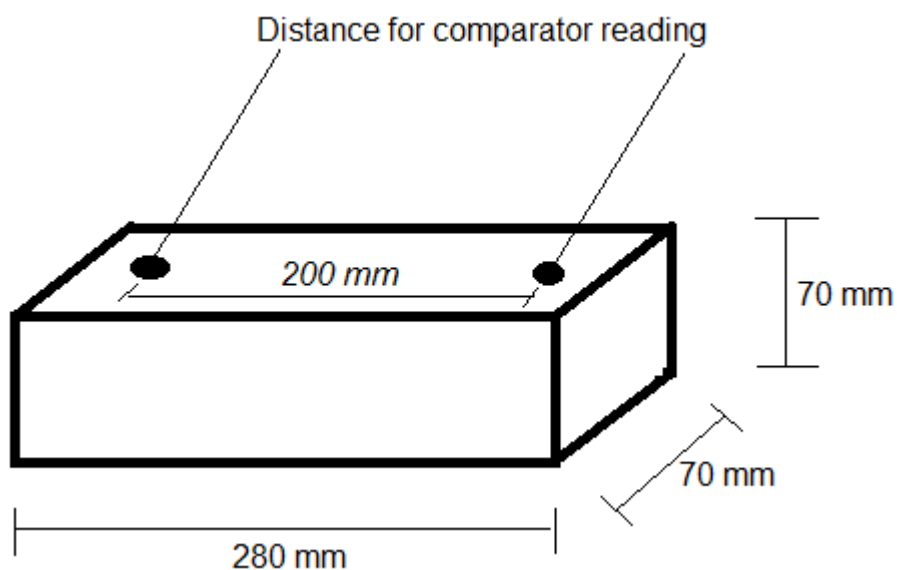
$$f_t = \frac{2P}{\pi DL} \quad (3.3)$$

In this case, f_t is the tensile strength in MPa whereas P is the maximum load applied in N, D and L the diameter and the length of the cylindrical specimen in mm. The results given rely on the average of three samples in the study.

3.6 Tests for Physical Properties

3.6.1 Drying Shrinkage and Weight Loss

Three 70x70x280 mm prism in respect to (ASTM C 157, 2008) to help in observation of drying shrinkage and the loss in weight of high strength concrete as illustrated in figure 3.11. When the prism being remolded is over then there was fixing of the gage length on each specimen using glued pins on the face of prisms. Measurement of the length change is carried out through a dial gage extensometer having a quantity of 200mm gage length with 0.002 strains for measuring. Notably, the measurements were carried out in the first three weeks in every 24 hours and later three times a week. Besides, identical prisms were used to determine the loss in weight. Additionally there were a variety of the drying shrinkage strain and the loss in weight in a respective period of 60 days in drying at $23\pm 2^{\circ}\text{C}$ and a relative humidity of 50 ± 5 percentage. Evaluation of various test results was done in relation to the average measurement of three respective prism specimens.





(b)

Figure 3.11 Free shrinkage test a) Free shrinkage test set up and b) Test specimens

3.6.2 Autogenous Shrinkage

Determination of different autogenous deformation was done by carrying out measurements on displacements and sealed concrete specimens. This study involves the autogenous deformations being measured on prism specimens having $70 \times 70 \times 280$ mm. From the written process there is inserting of two respective layers of plastic sheets in the mold before casting is carried out. After setting time of four approximate hours that results to sidewalls being de-molded then the stainless steel studs were settled on specimens by using a thin layer of adhesive. These measurements were taken above gage length of 200 mm (Figure 3.12).

The extensometer used in the measurements was equipped with a comparator with an accuracy of 0.001 m/m. The specimens were stored in a room at $20 \pm 2^\circ\text{C}$ and 65% RH. Immediately after de-molding at 24 hours, each specimen was sealed using two

layers of plastic sheets and with a layer of aluminum foil (Figure 3.13). Measurements were made according to the ASTM C 41 after 24 hours in the casting room. Specimens of each series were weighed at 1 and 28 days to monitor whether the sealing layers preserved RH in the specimens. Weight changes for all specimens in each series were not more than 0.08%.



Figure 3.12: a) Autogenous test specimens. b) Test apparatus

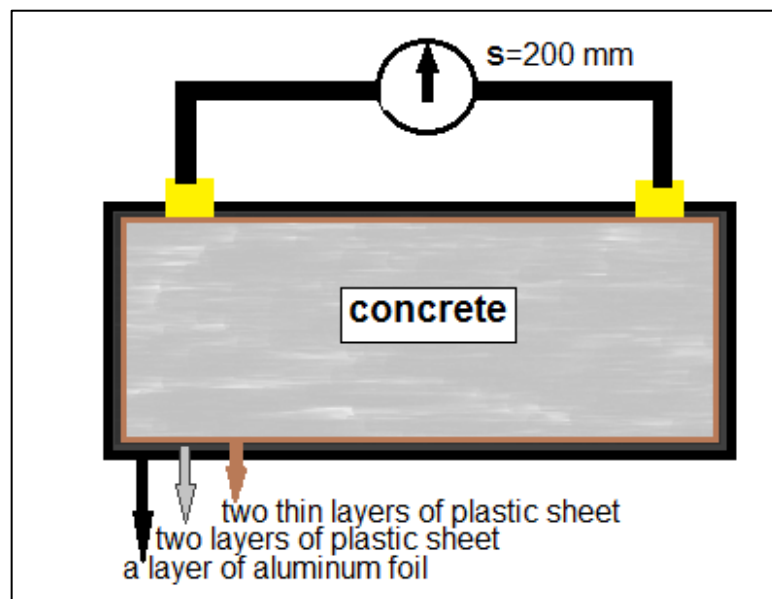


Figure 3.13 Autogenous deformation test set up for concrete specimens

3.6.3. Restrained Shrinkage Cracking

This study entails the utilization of the ring-shaped specimens with the need of determining the shrinkage that causes cracking of high strength concrete. From the ring dimensions in Figure 3.14, it is evident that an interior force resulting from the internal steel ring exposed to the concrete, and the variation will occurring between the values of the tensile hoop stress on the external and the internal surface of the ring specimen was about 10 percent. At the initial time, out of the maximum hoop only 20 percent the greatest rate of radial stress. Notably, this brought about chances of acceptance regarding the ring shaped specimen being exposed to uniaxial tensile stress that is uniform. This uniformity was accompanied with specimen being restrained by the steel ring having a thickness of 35mm that corresponds to four times greater than its width of 140 mm (Grzybowski and Shah, 1990; Shah et. al., 1992; Wiegrink, 1996).

Drying would occur only in the circumferential surface and this is necessitated by covering the concrete surface ring via a silicon rubber immediately after the removal of the outer mold of the ring specimen. (Figure 3.15). Thereafter there was subjection of the ring specimens to drying inside the cabinet with a respective relative humidity of 50 ± 5 percentage and a constant temperature of $23\pm 2^{\circ}\text{C}$ in accordance with (ASTMC157, 2008) in 60 days. To get the mean of the crack considering the mean of three evaluations was vital. One width is found at the midpoint of the ring then the other one is at the top of the ring, then finally the last one is at the bottom half of the ring (Figure 3.16). After the occurrence of the crack on the specimen surface there was, need to get the width of the crack in the first 7 days as every 24 hours besides every 48 hours.

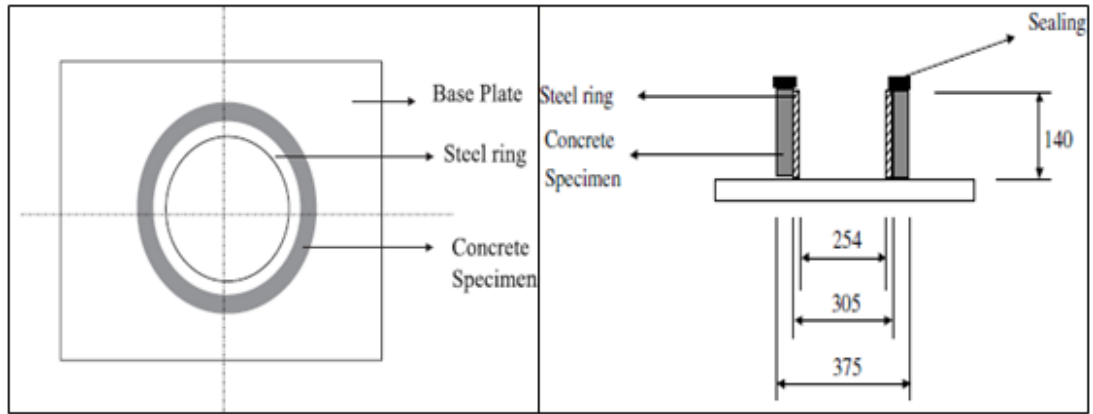


Figure 3.14 The dimension of restrained shrinkage ring specimen (in mm)



Figure 3.15 Restrained shrinkage test specimens



Figure 3.16 Photographic view of a cracked ring specimen

3.7. Microstructural Analysis

The investigations in the microstructural changes of the AA were realized by means of Scanning Electron Microscope (SEM) and EDX spectrum. The SEM is a new type of high- resolution microscope which allows the examination of the specimens in the presence of gases. As a result, wet or dry, insulating or conducting, and generally all specimens in their natural state can now be viewed with no or minimal preparation. Associated with the SEM photos, EDX spectrums were obtained to determine Ca and Si contents (Gesoglu et al., 2007).

CHAPTER 4

TEST RESULTS AND DISCUSSIONS

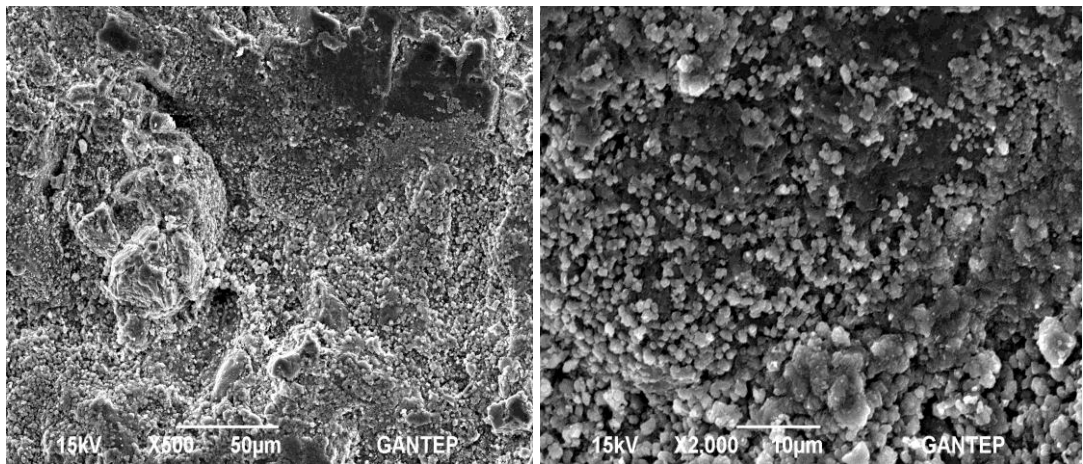
4.1. Fresh Concrete Density

Different amounts of a SP were applied to produce HSCs with slumps within the range of 150 ± 20 mm. The HSCs indicated a fresh density from 2325 to 2450 kg/m³ as shown in Table 4. The study showed that a decreased fresh density resulted from a rise in the level of replacement of ASA and AFA. For example, in comparison to AFA0ASA0, the control mixture having a fully natural aggregate; for AFA0ASA20 and AFA20ASA0, there was a decrease of 2.4% and 5.1% in the HSCs fresh density, respectively (Table 4). HSCs showed relatively high fresh densities in spite of the artificial aggregates used. This is attributable to the quite high specific gravity of the fly ash and the blast furnace slag that formed the artificial aggregates in addition to the high cement content and low w/c (Gesoglu et al., 2007; Gesoglu et al., 2006; Gesoglu et al., 2004).

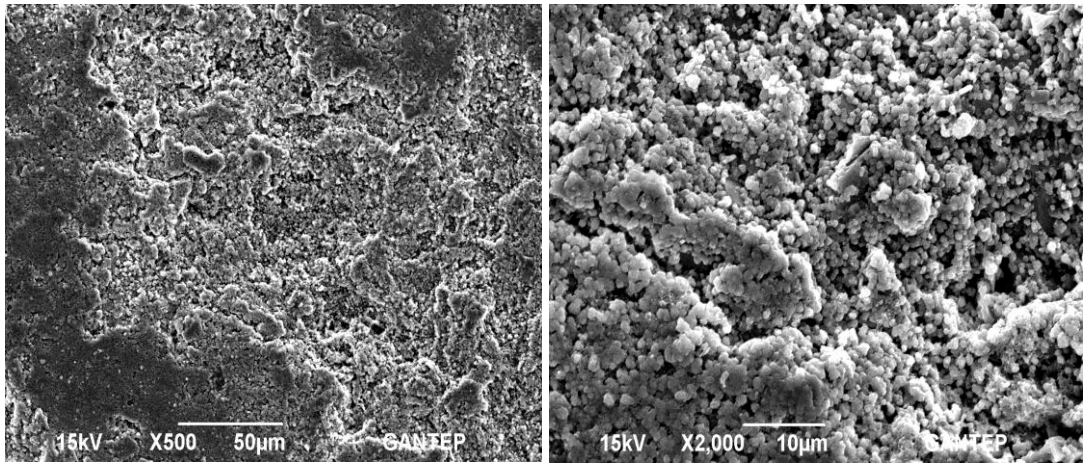
4.2. Microstructural Characteristics of ASAs and AFAs

Figure 4.1 indicates the changes in HSCs' cement paste matrix comprising of ASA and AFA. At comparatively high magnification of 500x, there was no clear difference observed between the interior structure of the AA and the outer shell from the SEM observation undertaken after 28 days. Faintly large pores were, however, observed in AFA0ASA20 and an inclusion of 20% ASA into the HSCs enabled

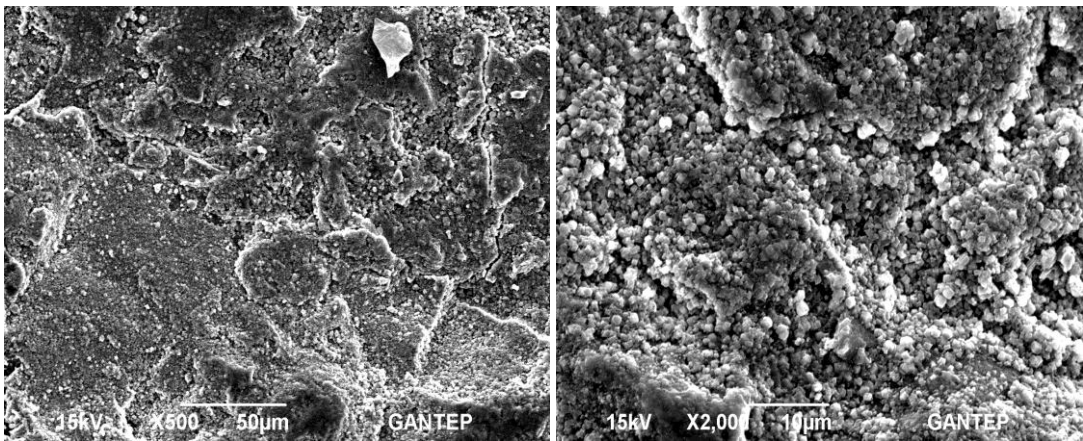
refinement of pores at a high magnification of 2000x. Reduced absorption of water was observed in this aggregate (ASA), probably owing to the dense outer shell (Gesoglu et al., 2007; Newman, 1993; Weber, 1997; TS EN 197-1, 2002). Seemingly, hydration products infiltrated the pores in the ASAs as evidenced by the large crystals formed in the pores (Wasserman and Bentur, 1996). The SEM-EDX for AFA0ASA0, AFA20ASA0 and AFA0ASA20 concretes largely influenced the composition of the hydrated phases, respectively (Figure 4.2, 4.3, and 4.4). Making the aggregate weaker, a low hydration rate occurred with lower C–S–H, along with a higher $\text{Ca}(\text{OH})_2$ content as indicated by the greater Ca peak, as this was overlooked in the AFA production stage. Nonetheless, as indicated by the greater Si peak in Figure 4.4 (Gesoglu et al., 2007), a higher hydration rate could have been realized with higher C–S–H for the HSCs containing ASA, had a greater CaO content and a comparatively greater specific surface density been used.



(a)



(b)



(c)

Figure 4.1 SEM observation of HSCs (a) control mix (b) HSCs incorporating AFA
(c) HSCs incorporating ASA

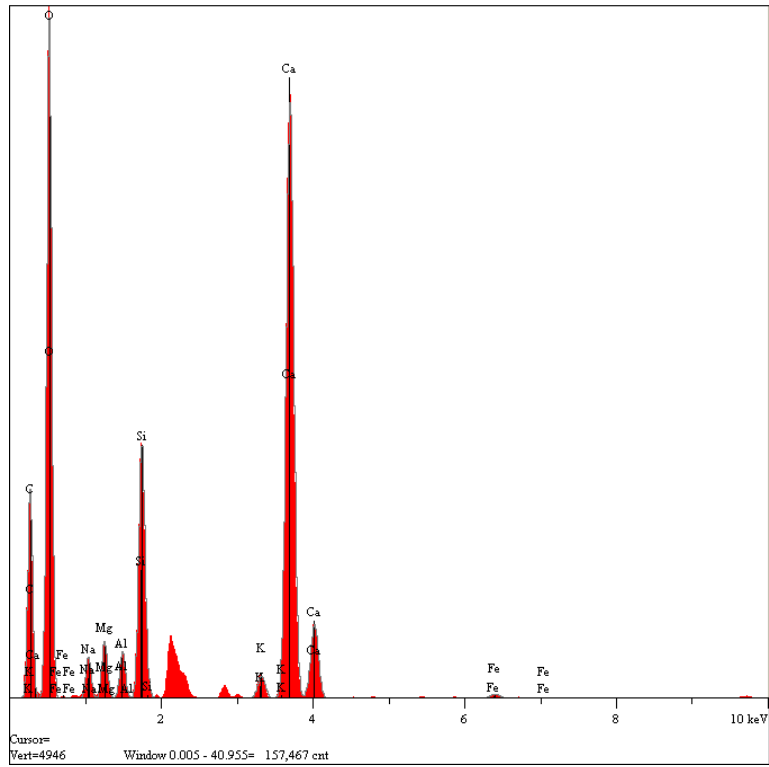


Figure 4.2 SEM-EDX for AFA0ASA0 and concretes

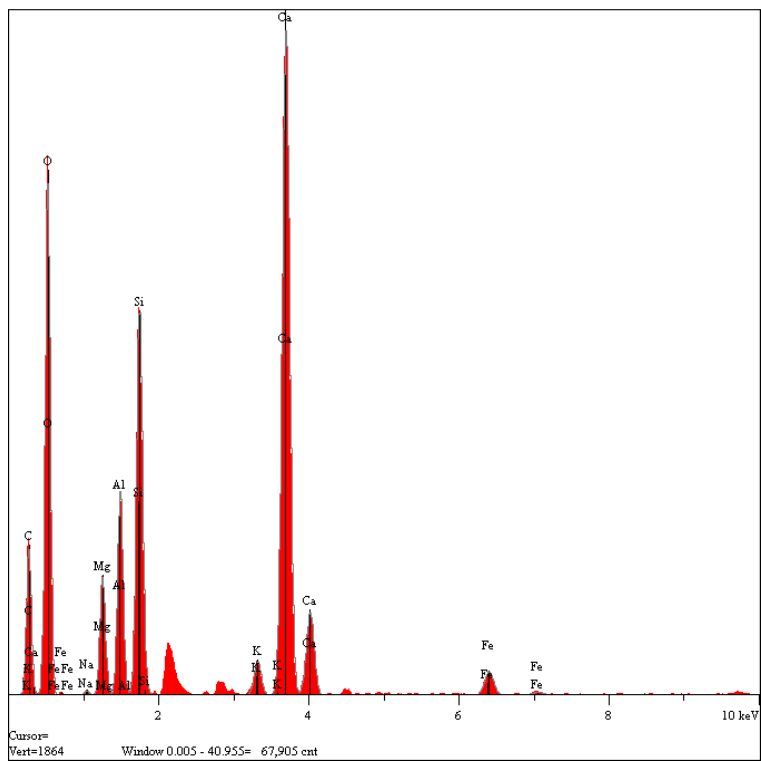


Figure 4.3 SEM-EDX for AFA20ASA0 concrete

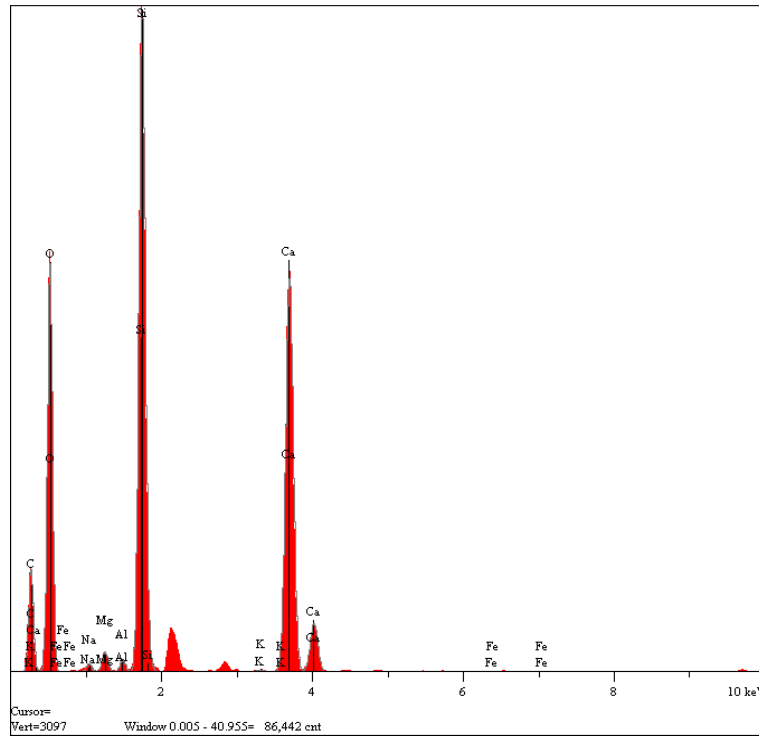


Figure 4.4 SEM-EDX for AFA0ASA20concrete

4.3. Mechanical Properties

4.3.1. Compressive Strength

Figure 4.5 and Figure 4.6, respectively, illustrate the effect of different AFA and ASA percentages on the splitting tensile and compressive strength of HSCs after 28 days. Regardless of the replacement level, increase in AFA content led to a noticeable decrease in the compressive strength of the concretes, whereas the HSCs containing ASAs had higher strength values to those of the control concrete. Also, while AFA20ASA0 had the smallest value of 65 MPa, HSCs with a 20% volume concentration of ASAs, alternatively, showed the highest compressive strength value, 76.5 MPa. This is to mean that, in comparison with AFA0ASA0, the control mix, the compressive strength of AFA0ASA20 increased by 7.5%. At a replacement level of 20%, on the contrary, the compressive strength decreased by 8.2% upon replacement of NWA with AFA. This is due to the use of a comparatively weak AFA to replace

NWA. It was noted that, however, the aggregate strength variances do not always account for the variance in the concrete strength.

Another factor influencing the concrete strength is the pozzolanic reaction occurring between the paste matrix and the aggregate. A secondary reaction between calcium from portlandite and the dissolved minerals resulting from the cold-bonded slag process are linked to the enhanced compressive strengths of HSCs containing ASAs. The silica in the aggregate is broken down by the hydroxyl ions, and thus reacting with the calcium contained in the portlandite, forming a CSH paste. The ASA and cement paste bond is thus further strengthened by this reaction. The slag thus becomes a real binder following a pozzolanic reaction anticipated to occur on this aggregate's surrounding phase, given that ASAs are porous in structure (Sivakumar and Gomathi, 2012). Ca(OH)_2 reacts with the slag components to form CSH which fills up empty spaces of the binding mediums, consequently strengthening the concrete structure; this happens at the hydration stage of the Portland cement (Mezghiche, 1999). In comparison to other HSCs, the compressive strength was improved due to the high content of silicon oxide in HSCs containing ASA as confirmed by an analysis carried out by SEM and EDX. Wasserman & Bentur also confirmed these results (Wasserman and Bentur, 1996). They stated that the general strength was influenced by the chemical and physical interfacial processes, beyond that of the aggregate strength.

4.3.2. Splitting Tensile Strength

The splitting tensile strength, as well, had comparatively similar behavior to that of compressive strength. While AFA20ASA0 had the lowest splitting tensile strength of 4.24 MPa, the highest was recorded for AFA0ASA20 being 4.74 MPa. The splitting tensile strengths revealed an inverse correlation with the volume ratio of AFA when increased gradually from 5% to 20% in relation to AFA0ASA0. When higher amounts are used, the AFAs intensify in the concretes' mechanical properties as they were weaker relative to the mortar phase (Gesoglu, 2004; Gesoglu et al., 2007; Manikandan and Ramamurthy, 2007; Ramamurthy and Harikrishnan, 2006). However, the increase in the aggregate crushing strength significantly reduced this opposite effect of ASAs in compressive strength, modulus of elasticity, splitting tensile strength.

4.3.3. Modulus of Elasticity

There were considerable similarities recorded between the observed elastic modulus behavior and that of the compressive strength. Subject to the level of replacement, HSCs containing ASA recorded the highest static elastic modulus (refer to Figure 4.7). At replacement levels of 5%, 10%, 15% and 20%, the modulus of elasticity of the concretes increased by 1.2%, 1.6%, 9.3% and 15.1% respectively, upon replacement of NWA with ASA. On the other hand, AFA5ASA0, AFA10ASA0, AFA15ASA0, and AFA20ASA0 concretes exhibited a 2.9%, 7.3%, 9.2% and 18.1% modulus of elasticity reduction for AFA.

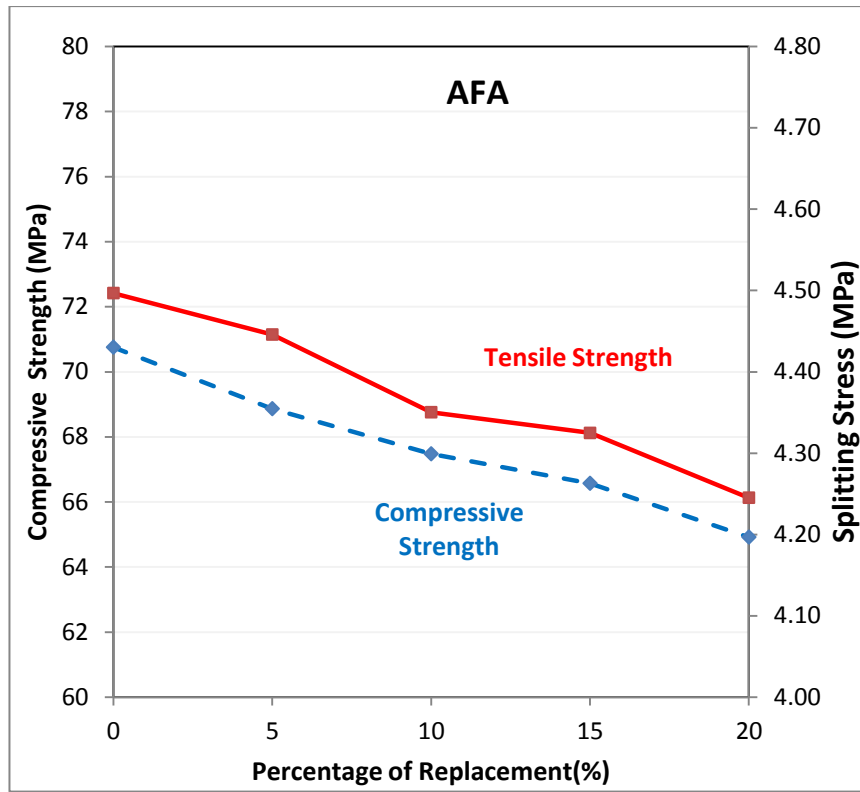


Figure 4.5 Variation of compressive/tensile strength of HSCs including AFA

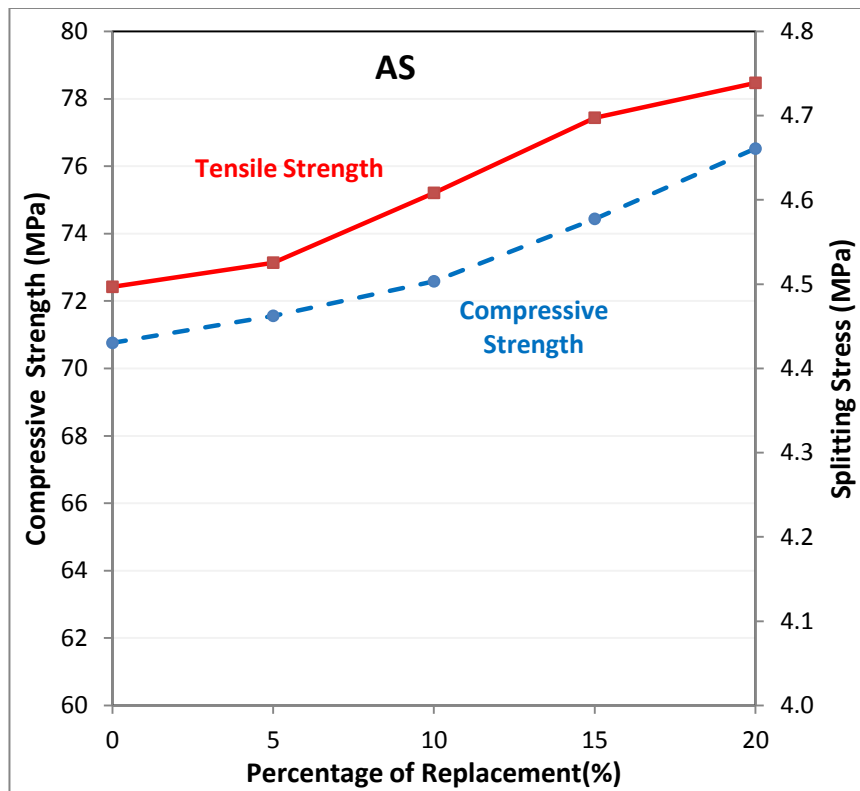


Figure 4.6 Variation of compressive/tensile strength of HSCs including ASA

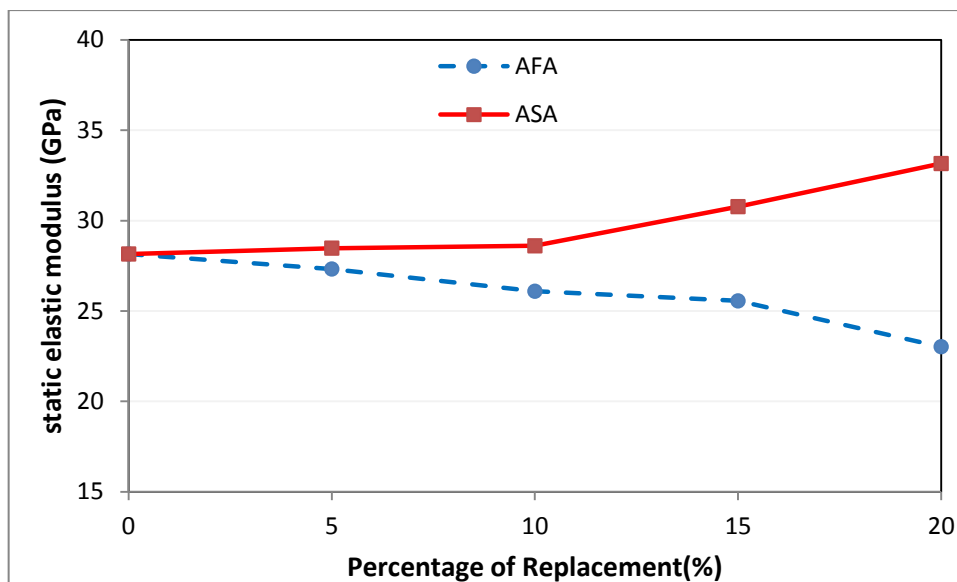


Figure 4.7 Variation of modulus of elasticity of all HSCs

4.4 Physical Properties

4.4.1 Drying Shrinkage and Weight Loss

Refer to Figure 4.8 and Table 4 for the effects of artificial aggregates on the differences in drying shrinkage with respect to time period for HSCs. In all mixtures, as time elapses, the rate of drying shrinkage gradually decreases. As justified by the increased drying shrinkage, great shrinkage strain in concretes is linked to high absorption properties in aggregates (Shah et al., 1992). In comparison to the control mixture, AFA5ASA0, AFA10ASA0, AFA15ASA0, AFA20ASA0 mixtures, for instance, showed a 3%, 4%, 5% and 7% upsurge in drying shrinkage, respectively. In general, the NWC shrinkage can be 50% less than that of concrete containing AA. The drying shrinkage in the HSCs-containing ASA was around 472 to 495 microstrain after 57 days as compared to 505 microstrain in the control mixture. The lowest shrinkage in AFA0ASA20 mix over the age of 57 days is found to be 7% lower than those in AFA0ASA0 mix (control mixture). This behavior was attributed to the variation in the water absorption and the crushing strength of the lightweight

aggregates used, but the effect of the latter was more pronounced (Gesoglu et al., 2004). High initial drying shrinkage and relatively low tensile strength may lead to the danger of shrinkage cracking for HSCs with AFA. However, the danger of shrinkage cracking can be compensated by the lower modulus of elasticity of HSC incorporating AFA (Khandaker and Anwar Hossain, 2004). Figure 4.9 illustrates the effects of weight loss resulting from the drying of HSCs with respect to time; while HSCs containing AFA showed greater loss in weight relative to the control mixture, HSCs containing ASA showed less weight loss, similar to in the drying shrinkage test results. After 10 days of the 57 days drying period, it was possible to distinguish the weight loss differences between ASA and AFA containing concretes. Even though the AFA aggregates employed were in SSD condition, increase in coarse aggregates resulted in increased loss of water which consequently led to a resultant increase in the unit water content.

Table 4 Drying, autogenous and restrained shrinkage performance with fresh density of HSCs

Mix code	Fresh Density	Weight loss (%)	Free Shrinkage microstrain	Autogenous Shrinkage microstrain	Average cracking age (day)	Max Crack Width (mm)
AFA0ASA0	2449.9	1.14	505	230	10	0.95
AFA5ASA0	2425.3	1.18	518	222	11	1.00
AFA10ASA0	2400.8	1.23	525	211	12	1.10
AFA15ASA0	2367.5	1.26	530	196	14	1.20
AFA20ASA0	2325.3	1.30	542	181	16	1.25
AFA0ASA5	2448.5	1.11	495	227	11	0.93
AFA0ASA10	2432.2	1.07	490	220	12	0.90
AFA0ASA15	2405.8	1.06	480	215	13	0.86
AFA0ASA20	2391.3	1.03	472	212	15	0.82

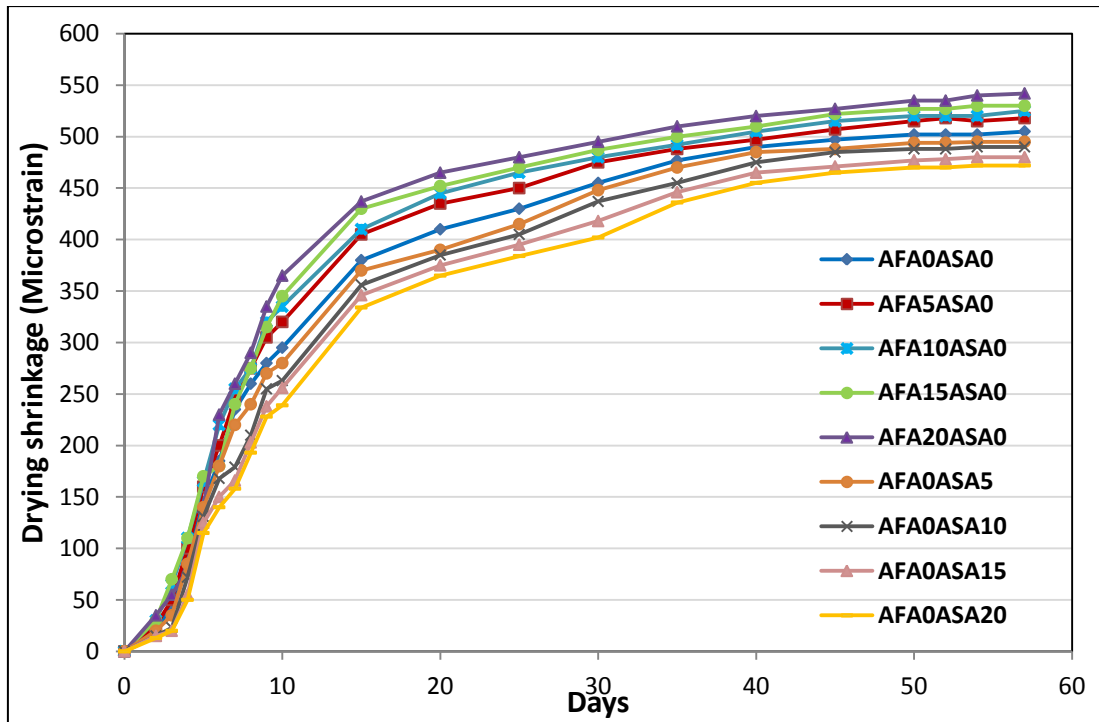


Fig. 4.8 drying shrinkage for HSCs mixtures

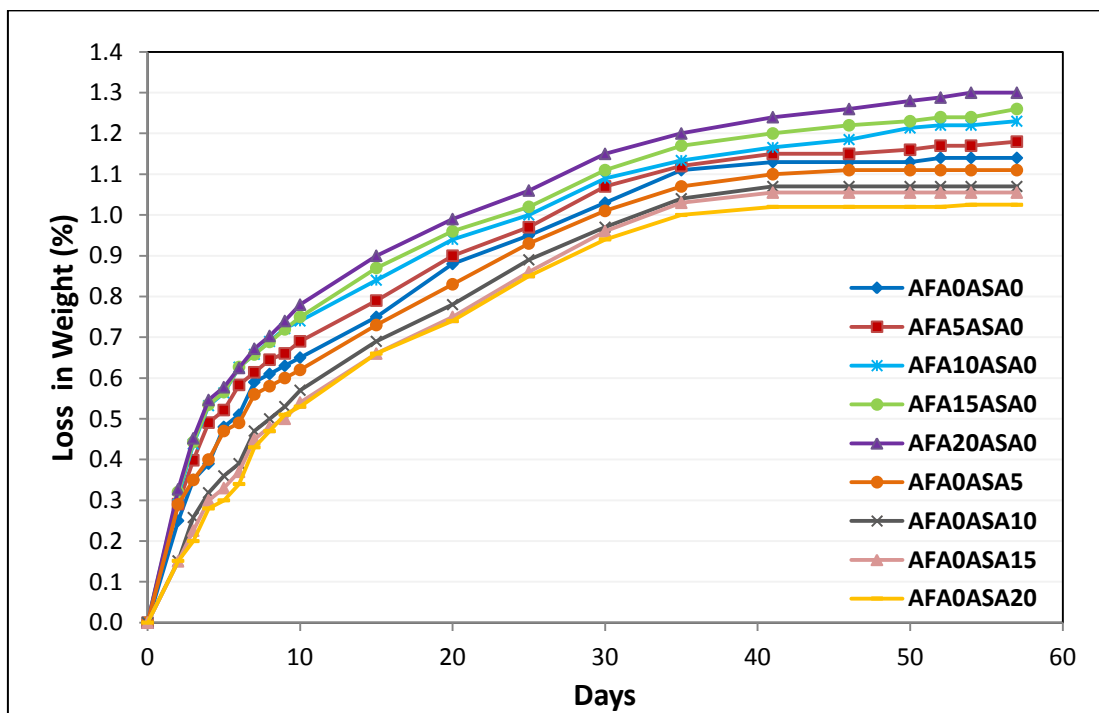


Fig. 4.9 Weight loss for HSCs mixtures

4.4.2 Linear Autogenous Shrinkage

According to Jensen & Hansen, autogenous deformation refers to “the bulk deformation of cementitious material without any weight loss when cement hydrates in a closed, isothermal system not subject to external forces” (Jensen and Hansen, 2001). Autogenous deformation occurs after the relative humidity of the cement paste decreases. After sometime, the main component of autogenous deformation becomes the self-desiccation shrinkage (Akçay, 2007). Table 4, Figure 4.10 show the measurement of the linear autogenous deformation of the HSCs for a period of 57 days. In the AFA0ASA0 (control mix), 230 microstrain was recorded as the autogenous shrinkage. When the normal weight aggregate is replaced by AFA, the linear autogenous shrinkage of HSCs at 57 days was mitigated by 3.47%, 8.26%, 14.78 and 21.3%, for AFA5ASA0, AFA10ASA0, AFA15ASA0, AFA20ASA0 mixes, respectively. However, for HSCs containing ASA, linear autogenous shrinkage decreased by as much as 1.3%, 4.4%, 6.5% and 7.8% for AFA0ASA5, AFA0ASA10, AFA0ASA15, and AFA0ASA20 mixes, respectively, compared with the control mixture. As an internal curing method, the lightweight aggregate water content and effect on the reduced restraining stresses and autogenous shrinkage in HSC is a clear demonstration on their efficiency (Gesoglu et al., 2004). Early researches came up with the same observations (Bentur et al., 2001; Khayat et al., 2013). Substantial decrease in the autogenous shrinkage magnitude of HSC resulted when the normal weight aggregates were used to replace even air-dried fine artificial LWAs as demonstrated by Bentur et al. (Bentur et al., 2001). In the study of Khayat et al, (Khayat et al., 2013) also concluded that a partial replacement of normal-weight aggregate by volume of saturated lightweight aggregate was very effective in eliminating the autogenous shrinkage and restrained stresses of the

normal-weight concrete. These results clearly expound that the internal drying of the concrete pores due to hydration generates a driving force by which water is transported from the pores of the lightweight aggregate into the partially dried pores of the cementitious matrix. The mechanisms of this transport process may be associated with capillary effects since the pores in the paste matrix are considerably smaller than those of the lightweight aggregate, and, as a result, capillary suction may take place (Bentur et al., 2001). However, AFAs were much more effective than ASAs on the mitigating autogenous shrinkage because of high internal supply water comes from high-water absorption capability of AFA. Accordingly, it is important to know the saturation degree and also the amount of desorption of LWA (Lura et al., 2003).

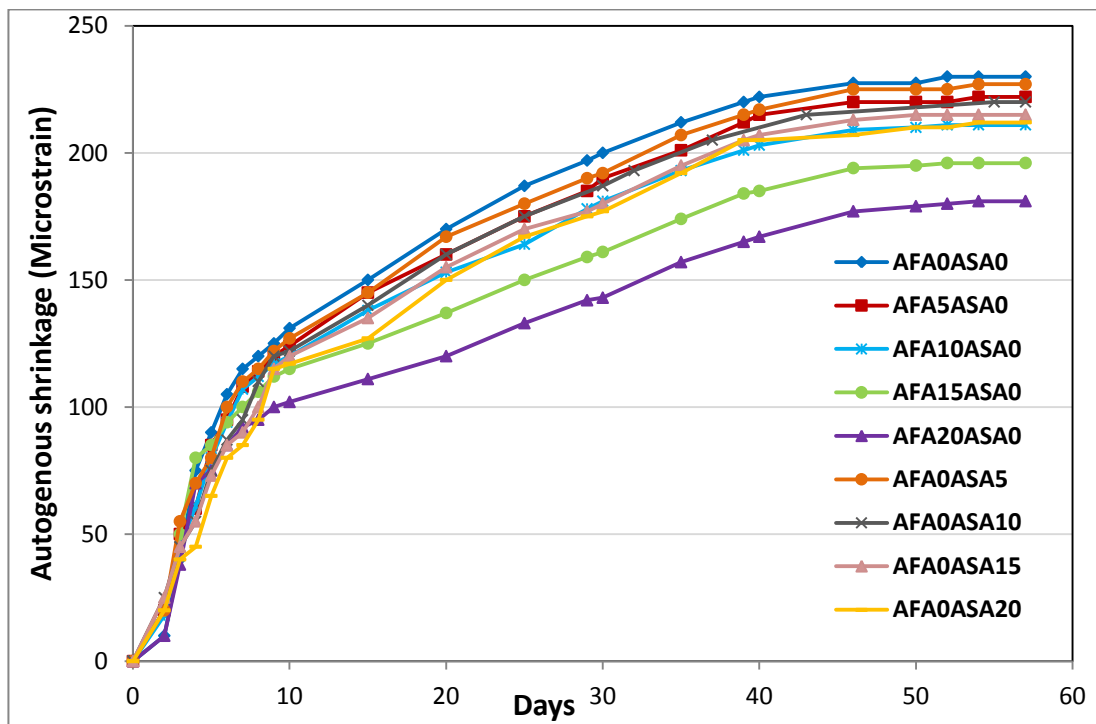


Figure 4.10 Autogenous shrinkage for HSCs contain ASAs & AFAs

4.4.3 Restrained shrinkage cracking

Concrete is expected to crack whenever the tensile stress induced by the constraint for the free shrinkage surpasses its tensile strength. Shrinkage cracking age and the maximum crack width of HSCs are given in Table 4, and the crack developments of the restrained shrinkage specimens are shown in Figure 11. There was a marked effect of AA type on the restrained shrinkage cracking performance of HSCs. As it can be seen from the table and figure that initial cracking of the specimen was observed at 10th day for control, however, the crack initialization of AFA20ASA0 and AFA0ASA20 concrete was observed to occur at 15th and 16th days, respectively. Despite the fact that AFA15ASA0 and AFA20ASA0 concretes had higher free shrinkage and lower tensile strength, the cracking time was extended 1 day than AFA0ASA15 and AFA0ASA20, respectively. Although AFAs provided water into the drying matrix at the very early ages and thus extended the cracking time by reducing the autogenous shrinkage, higher unit water content resulted in higher shrinkage values at later ages (Gesoglu et al., 2004). Furthermore, the lower elastic moduli of HSCs with AFAs helped in extending the cracking time with respect to HPCs with ASAs. In addition to the cracking time, the artificial aggregate type also influenced the final crack width associated with the reduction in the final shrinkage. Though the cracking time was extended, the crack opening for HSCs with AFA was faster in the first day due to the weakness of AFAs. The lowest crack propagation was observed for control mixture irrespective of drying time while the maximum crack widths at the end of 57 days were found to be 1.25 mm for AFA20ASA0. On the other hand, considering the overall drying period, HSCs incorporating with AFAs exhibited higher crack propagation with respect to AFA0ASA0. Nevertheless, the replacement of ASA with the natural aggregate

provided 2.1%, 5.2%, 9.5% and 13.6% reduction in the crack width for AFA0ASA5, AFA0ASA10, AFA0ASA15 and AFA0ASA20, respectively. The reduction observed in the cracking width for HSCs with ASAs mostly resulted from the reduced free shrinkage and the increased tensile strength as well as the higher modulus of elasticity.

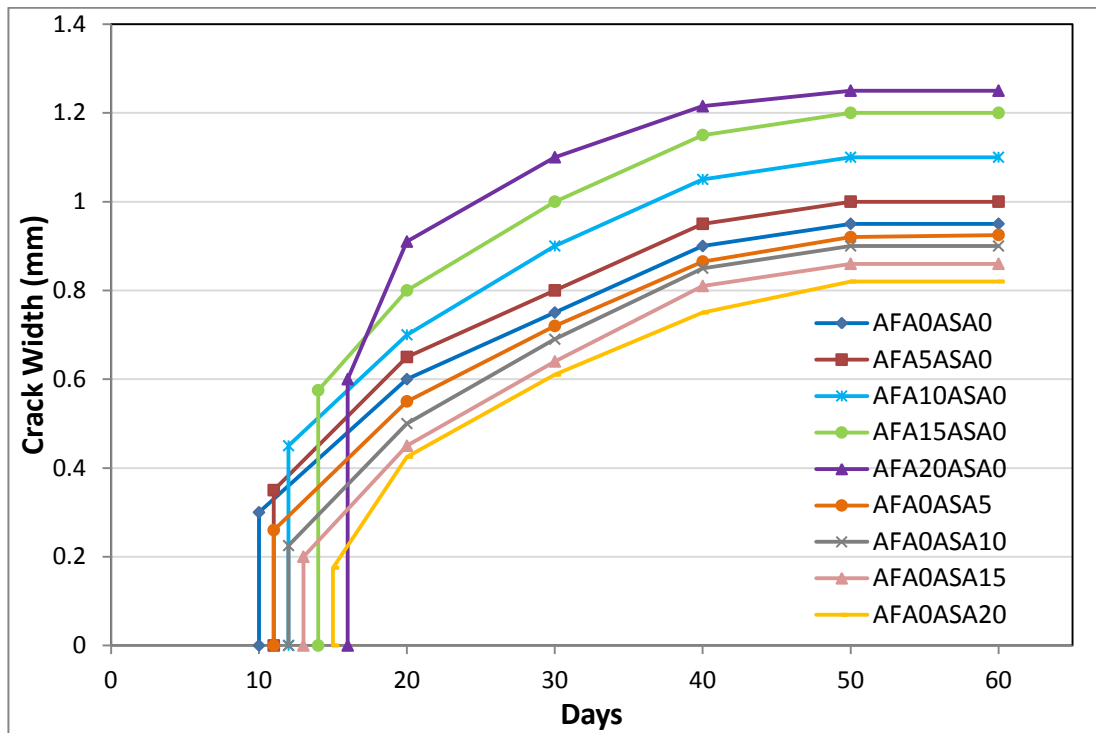


Figure 4.11 Restrained shrinkage cracking of HSCs

CHAPTER 5

CONCLUSIONS

Based on the findings of the study, the following conclusions may be drawn:

1. Increasing the replacement level of AFA and ASA resulted in a reduction of fresh density. Despite the usage of artificial aggregates, the fresh densities seem to be slightly high for HSCs.
2. All of the HSC mixtures were designed to give a slump of 150 ± 20 mm, which was achieved by adjusting the dosage of the super plasticizer used for the trial batches. In order to stay within the limits of the targeted slump, the amount HRWRA was decreased with the increase in AFA and ASA replacement level.
3. From SEM observation carried out at 28 days, at high magnification (2000x), there were slightly large pores in AFA0ASA20 while a pore refinement was provided by 20% inclusion of ASA into HSCs.
4. There was a marked reduction in the compressive strength of the concretes with increasing AFA content while HSCs having ASAs had comparable strength values to that of the control concrete, irrespective of the replacement level.
5. The static elastic modulus was the highest for HSCs with ASA, depending on the replacement level. While, AFA caused a decrease in modulus of elasticity.

6. The splitting tensile strength exhibited a similar pattern with compressive strength. Indeed, AFA0ASA20 and AFA had the highest splitting tensile strengths of 4.74 MPa whereas the lowest was measured as 4.24 MPa for AFA20ASA0.
7. Drying shrinkage rate is reduced gradually with the time passed for all mixtures. There was an increase in drying shrinkage by as high as 3%, 4%, 5% and 7% for AFA5ASA0, AFA10ASA0, AFA15ASA0, AFA20ASA0 mixes, respectively, compared to control mixture. While, drying shrinkage of HSCs with ASAs changed between 472 and 495 microstrain compared to about 505 microstrain in control mixture.
8. HSCs incorporated with ASAs indicated lower weight loss whereas HSCs including AFAs exhibited higher weight loss in comparison with control mixture.
9. When the normal aggregate is replaced by AFA, the linear autogenous shrinkage of HSCs at 57 days was mitigated by 8.26% and 21.3%, for AFA10ASA0 and AFA20ASA0 mixes, respectively. However, for HSCs containing ASA, linear autogenous shrinkage decreased by as much as 4.4% and 7.8% for AFA0ASA10 and AFA0ASA20 mixes, respectively, compared with the control mixture.
10. In spite of mixes containing ASA cracked earlier than concretes with AFA, maximum crack width for this concrete poorer than other mixes. The crack initialization of AFA20ASA0 and AFA0ASA20 concrete was observed to occur at 15th and 16th days, respectively.
11. HSCs incorporating with AFAs exhibited higher crack propagation with respect to control mixture. Nevertheless, the replacement of ASA with the natural aggregate provided 5.2% and 13.6% reduction in the crack width for AFA0ASA10 and AFA0ASA20, respectively.

REFERENCES

AASHTO-LRFD, AASHTO LRFD. (2004). Bridge Design Specifications. Third Edition ed. Washington: *American Association of State Highway and Transportation Officials*.

ACI Committee 318 (1999). Building Code Requirement for Reinforced Concrete (ACI 318-99) and Commentary (ACI 318R-99). *American Concrete Institute, Farmington Hills, Mich.*, 391 pp.

ACI Committee 363 (ACI 363R-10) (2010). State-of-the-Art Report on High Strength Concrete. *American Concrete Institute, Detroit, Michigan*, 55 pp.

ACI Committee 232. (1996). Use of Fly Ash in Concrete. *American Concrete Institute, USA*.

ACI Committee 116. (2000). Cement and Concrete Terminology, in ACI Manual of Concrete Practice. *American Concrete Institute: Farmington Hills, MI*. p. 116R.1-116R.73.

ACI Committee 209. (1997). Prediction of Creep, Shrinkage, and Temperature Effects in Concrete Structures, in ACI Manual of Concrete Practice. *American Concrete Institute: Farmington Hills, MI*. p. 209R.1-209R.47.

ACI. (2010). ACI Concrete Terminology. American Concrete Institute. *Farmington Hills, MI*.<http://terminology.concrete.org> (accessed June 6, 2013).

ACI Committee 213. (2003). Guide for Structural Lightweight-Aggregate Concrete, in ACI Manual of Concrete Practice. *American Concrete Institute: Farmington Hills, MI*. p. 38.

Aïtcin, P.-C., A.M. Neville, and P. Acker. (1997). Integrated view of shrinkage deformation. *Concrete International*, 19(9). p. 35-41.

Aïtcin, P.-C. (1998). High-performance concrete. *London; New York: E. & F.N. Spon*, xxxii, 591.

Akçay, B., Pekmezci, B.Y. and Tasdemir, M.A. (2005). Utilization of artificial lightweight aggregates in hardened cement paste for internal water curing, *Proc. of fib Keep Concrete Attractive, Budapest, 23-25 May, Eds., Balazs and Borosnyoi*, 1, pp 374-380.

ASTM C618–08. Standard Specification for Coal Fly Ash and Raw or Calcined Natural Pozzolan for Use in Concrete. ASTM International. *Annual Book of ASTM Standards*.

ASTM C 989. (1999). Standard Specifications for Ground Granulated Blast–Furnace Slag for Use in Concrete and Mortars. The American Society for Testing and Materials, Pennsylvania. *Annual Book of ASTM Standards*.

ASTM C127. (2007). Standard test method for specific gravity and absorption of coarse aggregate. *Annual Book of ASTM Standards*.

ASTM C496 / C496M - 11. (2012). Standard Test Method for Splitting Tensile Strength of Cylindrical Concrete Specimens. International standards worldwide. *Annual Book of ASTM Standards*.

ASTM C157. American Society for Testing and Materials. (2008). Standard test method for length change of hardened hydraulic-cement mortar and concrete. *Annual book of ASTM standards*, vol. 04.02. West Conshohocken, PA: ASTM.

Bentz, D.P. and Snyder, K.A. (1999). Protected paste volume in concrete extension to internal curing using saturated lightweight fine aggregate, *Cement and Concrete Research*, 29, 1863–1867.

Bentur, A., Igarashib, S-I. and Kovler, K. (2001). Prevention of autogenous shrinkage in high-strength concrete by internal curing using wet lightweight aggregates, *Cement Concrete Research*, 31, 1587–1591.

Bayat, O. (1998). Characterization of Turkish Fly Ashes. *ELSEVIER, Fuel*, Issues 9–10, V.77, pp.1059–1066, July–August 1998.

Bijen, J. (1996). Blast Furnace Slag Cement. *Association of Netherlands Cement Industry*.

Bijen, J. (1986). Fly Ash Aggregates. *ACI SP 79-26, American Concrete Institute*.

Bijen, J. M. (1986). Manufacturing processes of artificial lightweight aggregates from fly ash. *International Journal Cement Composite and Lightweight concrete*, V.8, pp.191-199.

Barksdale, R. D. (1993). The Aggregate Handbook. *National Stone Association*.

Bijen, J. M. and de Rooij, M. (1999). Aggregate–Matrix Interfaces. *International Conference on Concretes, Dundee, Scotland*.

Bazant, Z.P. and S. Baweja. (1995). Creep and Shrinkage Prediction Model for Analysis and Design of Concrete Structures - Model B3, RILEM Draft Recommendation. *Materials and Structures*, 28. p. 357-365.

Bentz, D.P., & Weiss, W.J. (2011). Internal curing: A 2010 state-of-the art review. (NISTIR 7765). *U.S. Department of Commerce, National Institute of Standards and Technology*.

Bentz, D.P, Lura, P, & Roberts, J.W. (2005). Mixture proportioning for internal curing. *Concrete International*, 27(2), 35-40.

Bentz, D.P., & Snyder, K.A. (1999). Protected paste volume in concrete extension to internal curing using saturated lightweight fine aggregate. *Cement and Concrete Research*, 29, 1863-1867.

Bentz, D.P., & Weiss, W.J. (2011). Internal curing: A 2010 state-of-the art review. (NISTIR7765). *U.S. Department of Commerce, National Institute of Standards and Technology*.

Bentz, D.P. and K.A. Snyder. (1999). Protected paste volume in concrete - Extension to internal curing using saturated lightweight fine aggregate. *Cement and Concrete Research*, 29(11). p. 1863-1867.

Berntsson, L.; Chandra, S. and Kutti, T. (1990). Principles and Factors Influencing High-Strength Concrete Production, *Concrete International*, December, pp.59-62.

BSI 1881-121: (1983). Testing Concrete - Part 121: Recommendations for the Measurement of Static Modulus of Elasticity. *BSI: British Standards Institution*, Jan 31, 1983.

BS 1881-116: (1983). Method for determination of compressive strength of concrete cubes, *Gibb Limited, Jacobs Gibb Ltd*, 24 December 2003.

Cano Barrita, F.d.J., T.W. Bremner, and B.J. Balcom. (2002). Use of Magnetic Resonance Imaging to Study Internal Moist Curing in Concrete Containing Saturated Lightweight Aggregate in High Performance Structural Lightweight Concrete. *SP-218. Phoenix, AZ: American Concrete Institute*.p. 155-175.

Carreira, D.J. and R.G. Burg. (2000). Testing for Concrete Creep and Shrinkage. in The Adam Neville Symposium: Creep and Shrinkage - Structural Design Effects SP-194. *Atlanta: American Concrete Institute*.p. 381-420.

Comite Euro-Internacional du Beton (CEB) and Federation Internationale de la Precontrainte (FIP), *CEB Code Final Draft Section 3, Materials prEN 1992-1*. (2001). p. 25-31.

Castro, J., De la Varga, I., Goloas, M., & Weiss, J. (2010). Extending internal curing concepts(using fine LWA) to mixtures containing high volumes of fly ash. Achieving safe, smart& sustainable bridges : *Proceedings, 2010 Concrete Bridge Conference. Phoenix,Arizona, Feb. 24-26 2010*.

Carrasquillo, R. L. (1985). Production of High Strength Pastes, Mortars, and Concrete, Very High Strength Cement-Based Materials, *Materials Research Society Symposia Proceedings*, Vol. 42, pp.151-168.

Cheeseman, C. R., Makinde, A., Bethanis, S. (2005). Properties of lightweight aggregate produced by rapid sintering of incinerator bottom ash. *Resources, Conservation and Recycling*. 43(2), 147-162.

de Larrard, F., P. Acker, and R. Le Roy. (1994). Shrinkage, Creep and Thermal Properties, in High Performance Concrete: Properties and Applications, S.P. Shah and S.H. Ahmad, *Editors. McGraw-Hill: New York, NY.* p. 65-114.

Dhir, R. K. and Dyer, T. D. (1999). Modern Concrete Materials: Binders, Additions and Admixtures, *Thomas Telford Publishing, London, UK.*

Detwiler, R. J., Wenk, R. and Monteiro, P. (1988). Texture of calcium hydroxide near the aggregate cement paste interface. *Cement and Concrete Research Journal*, V. 18, Issue 5, pp.823-829.

Doven, A. G. (1996). Lightweight fly ash aggregate production using cold bonding agglomeration process. PhD Thesis, *Boğaziçi University, Turkey.*

Federation Internationale de la Precontrainte / Comite Euro-International du Beton (FIP/CEB) (1990). High Strength Concrete: State of the Art Report. *Bulletin d'Information No.197, London, UK*, 61 pp.

Gagne, R., Boisvert, A. and Pigeon, M. (1996). Effect of Superplasticizer on Mechanical Properties of High - Strength Concretes with and without Silica Fume. *ACI Materials Journal*, V. 93, No. 2, pp.111-120.

Gesoğlu, M. (2004). Effects of lightweight aggregate properties on mechanical, fracture, and physical behavior of lightweight concretes. PhD thesis, *Istanbul, Bogazici University.*

Goldstick, T. K. (1962). A Survey of the Literature Pertinent to Iron Ore Pelletizing. *In Agglomeration, Inter Science Publishers, New York*, pp. 1067-1104.

Gardner, N.J. and M.J. Lockman, Design provisions for drying shrinkage and creep of normal-strength concrete. *ACI Materials Journal*, 98(2): 2001. p. 159- 167.

Geiker, M.R., D.P. Bentz, and O.M. Jensen. (2002). Mitigating Autogenous Shrinkage by Internal Curing. in High Performance Structural Lightweight Concrete. *SP- 218. Phoenix, AZ: American Concrete Institute.*p. 143-154.

Grzybowski, M., Shah, S. P. (1990). Shrinkage cracking of fiber reinforced concrete. *ACI Materials Journal*. 87(2), 138-148.

- Gesoğlu M., Özturan T., Güneyisi E. (2004). Shrinkage cracking of lightweight concrete made with cold-bonded fly ash aggregates. *Cement and Concrete Research*. 34, 1121-1130.
- Gesoğlu, M., Güneyisi, E., Öz, H. Ö. (2012). Properties of lightweight aggregates produced with cold-bonding pelletization of fly ash and ground granulated blast furnace slag. *Materials and Structures*. 45, 1535-1546.
- Gesoğlu M, Özturan T, Güneyisi E. (2006). Effects of cold-bonded fly ash aggregate properties on the shrinkage cracking of lightweight concretes. *Cement & Concrete Composites* 28, 598–605.
- Gesoğlu M, Özturan T, Güneyisi E. (2007). Effects of fly ash properties on characteristics of cold-bonded fly ash lightweight aggregates. *Constr Build Mater* 21:1869–1878.
- Hu, X.Z., and Wittman, F.H. (2000). Size effect on toughness induced by crack close to free surface. *Engineering Fracture Mechanics*, 65, 209-211.
- Henkensiefken, R., Nantung, T., & Weiss, J. (2011). Saturated lightweight aggregate for internal curing in low w/c mixtures: Monitoring water movement using x-ray absorption. *Strain*, 47, 432-441.
- Henkensiefken, R., Castro, J., Kim, H., Bentz, D., & Weiss, J. (2009). Internal curing improves concrete performance throughout its life. *Concrete InFocus*, 8(5), 22-30.
- Holt, E.E. (2001). Early age autogenous shrinkage of concrete (Vol. 446). *Technical Research Centre of Finland*.
- Holm, T.A., O.S. Ooi, and T.W. Bremner. (2003). Moisture Dynamics in Lightweight Aggregate and Concrete. in Theodore Bremner Symposium on High-Performance Lightweight Concrete. *Tessaloniki, Greece*.p. 167-184.
- Hoff, G.C. (2003). Internal Curing of Concrete using Lightweight Aggregate. In Theodore Bremner Symposium on High-Performance Lightweight Concrete. *Tessaloniki, Greece*.p. 185-203.

Hammer, T.A., Ø. Bjøntegaard, and E.J. Sellevold. (2002). Internal Curing - Role of Absorbed Water in Aggregates in High Performance Structural Lightweight Concrete. *SP-218. Phoenix, AZ: American Concrete Institute*.p. 131-142.

Holm, T.A. and T.W. Bremner, State-of-the-Art Report on High-Strength, High-Durability Structural Low-Density Concrete for Applications in Severe Marine Environments, in Innovations for Navigation Projects Research Program. *US Army Corps of Engineers. Engineer Research and Development Center, Structures Laboratory: Vicksburg, MS. (2000).*

Jaroslav, S., Ruzickova, Z. (1987). Pelletization of Fines. Ore Research Instituted-Prague, *Elsevier Science Publishing Company, New York.*

Jensen, O.M. and P.F. Hansen. (2001). Autogenous deformation and RH-change in perspective. *Cement and Concrete Research*, 31(12). p. 1859-1865.

Jensen, O.M. and P.F. Hansen. (2002). Water-entrained cement-based materials II. Experimental observations. *Cement and Concrete Research*, 32(6). p. 973- 978.

Jensen, O.M. and P.F. Hansen. (2001). Water-entrained cement-based materials I. Principles and theoretical background. *Cement and Concrete Research*, 31(4). p. 647-654.

Jensen, O.M., & Lura, P. (2006). Techniques and materials for internal water curing of concrete. *Materials and Structures*, 39, 817-825.

Jensen, O.M. and P. Lura. (2003). Techniques for Internal Curing of Concrete. In *Advances in Cement and Concrete. Copper Mountain, Colorado: Engineering Conferences International*.p. 67-78.

Joseph G., Ramamurthy K. (2009). Influence of fly ash on strength and sorption characteristics of cold-bonded fly ash aggregate concrete. *Construction and Building Materials*. 23,1862-1870.

Kayali, O., Haque, M.N. and Zhu, B. (1999). Drying shrinkage of fibre-reinforced lightweight aggregate concrete containing fly ash, *Cement and Concrete Research*, 29, 1835-1840.

Kapur, P. C. (1978). Balling and Granulation. *Advances in Chemical Engineering, V. II*, Academic Press, New York, pp. 56-123.

Kapur P. C. and Fuerstenau, D. W. (1964). Kinetics of Green Pelletization, *Trans. AIME*, V. 229, pp. 348-355.

Kosmatka, S. H., Kerkhoff, B. and Panarese, W. C. (2002). Design and Control of Concrete Mixtures. *14th Edition, Portland Cement Association*.

Kohno, K., et al. (1999). Effects of artificial lightweight aggregate on autogenous shrinkage of concrete. *Cement and Concrete Research*, 29(4). p. 611-614.

Kovler, K. and O.M. Jensen. (2005). Novel Techniques for Concrete Curing – New Methods for low w/cm mixtures. *Concrete International*, 27(9). p. 39-42.

Ke, Y., Beaucour, A. L., Ortola, S., Dumontet, H., Cabrillac, R. (2009). Influence of volume fraction and characteristics of lightweight aggregates on the mechanical properties of concrete. *Construction and Building Materials*. 23, 2821-2828.

Lura, P., Bentz, D.P., Lange, D.A., Kovler, K. and Bentur, A. (2004). Pumice aggregates for internal water curing, *Proceedings of International RILEM Conference on the Advances in Concrete Through Science and Engineering, Illinois*, 21-24 arch.

Lura, P. O.M. Jensen & K. van Breugel (2002). Autogenous deformation and RH change in portland and Blast Furnace Slag cement pastes. *Proc. 3rd Int. Sem. on Self-desiccation and Its Importance in Concrete Technology, 15 June, Lund, Sweden*, pp. 127-137.

Luke, K. (2002). Pulverized Fuel Ash as a Cement Extender. *In Structure and Performance of Cements 2nd Edition Spon Press, London*.

Lee, A. R. (1974). Blast furnace and Steel Slag: Production, Properties and Uses. *Edward Arnold Ltd, London*.

Lura, P., D.P. Benz, and D.A. Lange. (2003). Measurements of Water Transport from Saturated Pumice Aggregates to Hardening Cement Paste. in *Advances in*

Cement and Concrete. *Copper Mountain, Colorado: Engineering Conferences International*.p. 89-99.

Li, Y., Wu, D., Zhang, J., Dhang, L., Wu, D., Fang, Z., Yahua, S. (2000). Measurement and statistics of single pellet mechanical strength of differently shaped catalysts. *Powder Technology*. 113(1-2), 176-84.

Mehta, P. K. and Aïtcin, P.-C. (1990). Principles Underlying Production of High-Performance Concrete, *Cement, Concrete, and Aggregates, ASTM*, Vol. 12, No. 2, Winter, pp. 70-78.

Mindess, S., Young, J., and Darwin, D. (2003). Concrete. *Upper Saddle River, NJ:Prentice Hall*. p. 429-430.

Mehta, P. K. (2000). Reflections on Recent Advancements in Concrete Technology. *Second International Symposium on Cement and Concrete Technology*, V.1, pp.43-57.

Mehta, P.K. and P.J.M. Monteiro. (1993). Concrete : microstructure, properties, and materials. *2nd ed: McGraw-Hill*.

Mangialardi, T. (2001). Sintering of msw fly ash for reuse as a concrete aggregate. *Journal of Hazardous Materials*. B87, 225-39.

Manikandan R, Ramamurthy K. (2007). Influence of fineness of fly ash on the aggregate pelletization process. *Cem Concr Comp* 29:456–464.

Mezghiche B, Guettela A, Chebili R, Zeghichi L. (1999). Study of the Effect of Alkalis on the Slag Cement Systems. *Proceedings of International Conferences on Modern Concrete Materials, Binders, Additions and Admixtures, Dundee, Scotland*. p. 287-93.

Naik, T. R., Singh, S.S., Hu, W. Y. (1992). High Volume Fly Ash Concrete Technology. *Research Project of Center for By-Products Utilization, University of Wisconsin-Milwaukee*.

Neville, A .M. (2004). Properties of Concrete. *Pearson Prentice Hall, Essex*.

- Nagataki, S. and Sakai, E. (1994). Applications in Japan and South East Asia, In High Performance Concretes and Applications, edited by S. P. Shah and S. H. Ahmad, *Edward Arnold, London*, pp. 375-397.
- Newman J.B. (1993). Properties of structural lightweight aggregate concrete, in: J.L. Clarke (Ed.), *Structural Lightweight Aggregate Concrete, Chapman & Hall, London*. pp. 19–44.
- Ozyildirim, C. (2003). Investigation of Self-consolidating Concrete. *Paper No. 01-345, TRB*.
- Powers, T.C., *Rev. Mater. Construct (Paris)*, (545). (1961). p. 79-85.
- Pietsch, W. (1991). *Size Enlargement by Agglomeration. New York: John Wiley and Sons*.
- Perry, C. and Gillott, J. E. (1977). The influence of mortar-aggregate bond strength on the behavior of concrete in uniaxial compression. *Cement and Concrete Research Journal*, V. 7, Issue 5, pp.553-564.
- Philleo, R. (1991). Concrete Science and Reality. in *Materials Science of Concrete II. Westerville, OH: American Ceramic Society*.p. 1-8.
- Peterman, M. B. and Carrasquillo, R. L. (1986). *Production of High Strength Concrete, Noyes Publications, Park Ridge, New Jersey, USA*, 278 pp.
- Regourd, M. M. (2004). Cements Made from Blast-furnace Slag. In *Leas Chemistry of Cement and Concrete, Hewlett Edition, Elsevier, Oxford*.
- Ramamurthy, K., Harikrishnan, K. I. (2006). Influence of binders on properties of sintered fly ash aggregate. *Cement Concrete Composite*. V.28, pp.33-38.
- Rumpf, H. (1962). The Strength of Granules and Agglomerates. *Agglomeration, Inter science, New York*, pp. 379-418.
- RILEM TC69 Subcommittee 1. (1988). Physical Mechanisms and their Mathematical Descriptions, in *Mathematical Modeling of Creep and Shrinkage of Concrete*, Z.P. Bažant, *Editor. John Wiley & Sons: New York*.

RILEM Technical Committee, Early Age Cracking in Cementitious Systems. *TC 181-EAS (2002)*. ed. A. Bentur, *Early age cracking in cementitious systems, RILEM, Cachan*, pp. 388.

RILEM Technical Committee, Internal Curing of Concrete. *TC-ICC. Statement of work (2002)*.

Roberts, J. (2006). High performance concrete enhancement through internal curing. *Concrete in Focus*, 55-59.

Sadouki, H. and Wittmann, F.H. (2001). Numerical Investigations on damage in cementitious composites under combined drying and shrinkage and mechanical load, *Proc. Fourth Int. Conference on Fracture Mechanics of Concrete and Concrete Structures (Framcos), de Borst et al. (Eds), Cachan, France*, 95-98.

Swamy, R.N. and Lixian, W. (1995). The ingredients for high performance, in *Proceedings of International Symposium on Structural Lightweight Aggregate Concrete, Eds. Ivar Holand et al., Sanderfjord, Norwegian Concrete Association, Oslo, 20-24 June*, 628-639.

Sastry, K. V. S. and Fuerstenau, D. W. (1977). Kinetics and Process Analysis of Agglomeration of Particulate Materials. *It Agglomeration '77, AIME, New York*, pp. 381-402.

Sastry, K. V. S. and Fuerstenau, D. W. (1973). Mechanisms of Agglomerate Growth in Green Pelletization. *Powder Technology, V. 7*, pp. 97-105.

Subramanian, S. (1999). Interfaces in concrete—Achieving performance. *International Conference on Concretes, Dundee, Scotland*.

Sakata, K. (1993). Prediction of Creep and Shrinkage, *Creep and Shrinkage of Concrete in Fifth International RILEM Symposium. Barcelona, Spain: RILEM*.p. 649-654.

Sakata, K., et al. (2001). Prediction Equations of Creep and Drying Shrinkage for Wide- Ranged Strength Concrete in Creep Shrinkage and Durability Mechanics of

Concrete and Other Quasi-Brittle Materials. *Cambridge, Massachusetts, United States: Elsevier*.p. 753-758.

Shah, S. P., Karaguler, M. E., Sarigaphuti, M. (1992). Effects of shrinkage reducing admixtures on restrained shrinkage cracking of concrete. *ACI Materials Journal*. 89(3), 289-295.

Sivakumar A, Gomathi P. (2012). Pelletized Fly Ash Lightweight Aggregate Concrete: A promising material. *J CivEng Construct Tech* 3(2):42-48.

Tasdemir, M.A., Tasdemir, C., Grimm, R. and König, G. (2002). Role of aggregate fraction in the fracture of semi-lightweight high strength concrete, *Proceedings of the 6th International Symposium on Utilization of High Strength/High Performance Concrete, Leipzig, June, 1453-1466*.

T.A. Hammer (1992). High strength LWA concrete with silica fume - Effect of water content in the LWA on mechanical properties. *Supplementary Papers in the 4th CANMET/ACI Int. Conf. On Fly Ash, Silica Fume, Slag and natural Pozzolans in Concrete, Turkey*, pp. 314-330.

Tazawa, E.-I. (1999). Technical Committee on Autogenous Shrinkage of Concrete, *Japan Concrete Institute, Japan Concrete Institute Committee report, in Proceedings of International Workshop Autoshrink'98, Ed. Tazawa, E.-I., Hiroshima, Japan, E&FN SPON, London, 13-14 June, 1-67*.

Tasdemir, M.A., Tasdemir, C., Grimm, R. and König, G. (2002). Role of aggregate fraction in the fracture of semi-lightweight high strength concrete, *Proceedings of the 6th International Symposium on Utilization of High Strength/High Performance Concrete, Leipzig, June, 1453-1466*.

Tazawa, E. and S. Miyazawa. (1995). Experimental-Study on Mechanism of Autogenous Shrinkage of Concrete. *Cement and Concrete Research*, 25(8). p. 1633-1638.

Tokyay, M. (1998). Characterization of Turkish Fly Ashes. *Turkish Cement Manufacturers Association, Ankara*.

TS EN 197-1.Cement- Part 1: Composition, specifications and conformity criteria for common cements. *Turkish Standards* (2002).

Weber, S. and Reinhardt, H.W. (1997). A new generation of high performance concrete: Concrete with autogenous curing, *Advanced Cement Based Materials*, 6, 59-68.

Whiting, D, and Dziedzic, W. (1979). Effects of Conventional and High-Range Water Reducers on Concrete Properties. *Portland Cement Association, R & D Bulletin* 107T.

Wittmann, F.H. (1982). Creep and Shrinkage Mechanisms. in Creep and Shrinkage in Concrete Structures. *Lausanne, Switzerland: John Wiley & Sons*.p. 129- 161.

Weber, S. and H.W. Reinhardt. (1997). A new generation of high performance concrete: Concrete with autogenous curing. *Advanced Cement Based Materials*, 6(2). p. 59-68.

Wiegrink, K., Marikunte, S. M., Shah, S. P. (1996). Shrinkage cracking of high strength concrete. *ACI Materials Journal*. 93(5), 409-415.

Weber S, Reinhardt H.W., *Adv. Cem. Based Mater.* 6 (2) (1997) 59– 68.

Wasserman R. and Bentur A. (1996). Interfacial Interactions in Lightweight Aggregate Concretes and their Influence on the Concrete Strength, *Cement & Concrete Composites* 18. 67-76.

Yang, C. C., Huang, R. (1998). Approximate Strength of Lightweight Aggregate using Micromechanics Method. *Advanced Cement Based Materials*, V.7, pp.133-138.

Yashima, S., Kanda, Y., Sano, S. (1987). Relationship between particle size and fracture energy or impact velocity required to fracture as estimated from single particle crushing. *Powder Technology*. 51(3), 227-282.

Zhutovsky, S., K. Kovler, and A. Bentur. (2002). Efficiency of lightweight aggregates for internal curing of high strength concrete to eliminate autogenous shrinkage. *Materials and Structures*, 35(246). p. 97-101.